Wall current calculations for an NSTX VDE

J. A. Breslau, J. Bialek, A.H. Boozer, and A. Bhattacharjee

Workshop on Theory and Simulation of Disruptions

Princeton, NJ

July 13, 2015

Outline

- Verification of M3D with the DSC test problem
  - Equilibrium & stability
  - Nonlinear saturation of free boundary kink
  - Nonlinear saturation of wall-touching kink
- NSTX VDE study
  - Experimental observations
  - M3D results
  - IVB results
- Conclusions

The DSC Test Problem

- Straight cylinder equilibrium, circular cross-section
  - Plasma minor radius at *r*=0.6, tile surface at *r*=0.7, ideal wall at *r*=1.0.
  - Tile surface behaves as a perfect insulator before plasma reaches it; perfect conductor thereafter.
  - Plasma interior $q \equiv 1.0$; edge q=0.75.
  - Plasma pressure low, flat; conductivity infinite.

- Evolve 1,1 external kink mode with 2D version of Disruption Simulation Code (**DSC**) called Cbwtk.
  - Implements Kadomtsev-Pogutse single helicity MHD model.
  - Eliminates inertia by replacing the momentum equation with

$$\rho \frac{d\mathbf{V}}{dt} \rightarrow \gamma \mathbf{V} = \lambda \vec{\xi}$$

DSC Results

Free boundary kink (FBK) with ideal wall

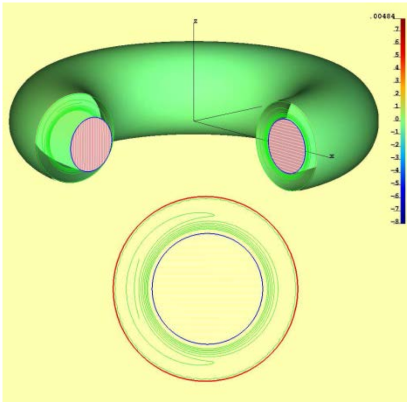

Initial perturbed plasma

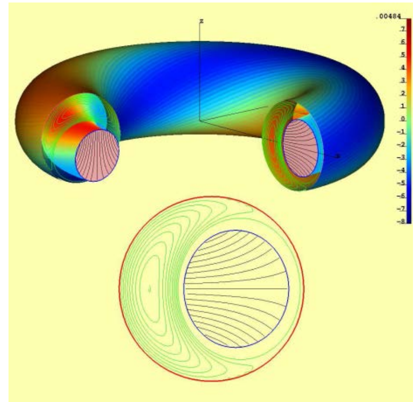

Fast phase of instability

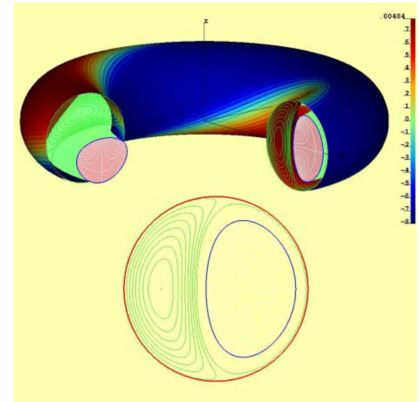

Saturation of the mode

Wall-touching kink (WTK) at tile surface

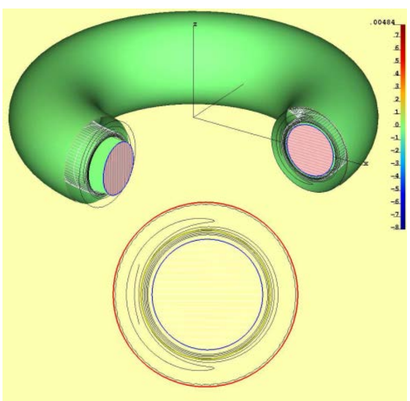

Initial perturbed plasma

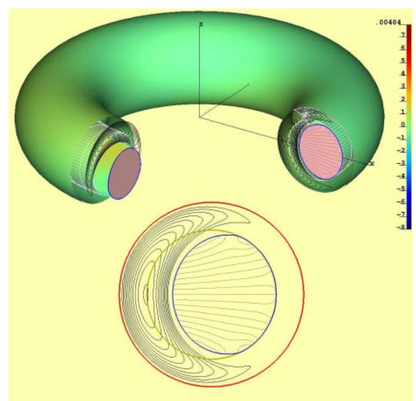

Fast phase of instability, excitation of Hiro currents

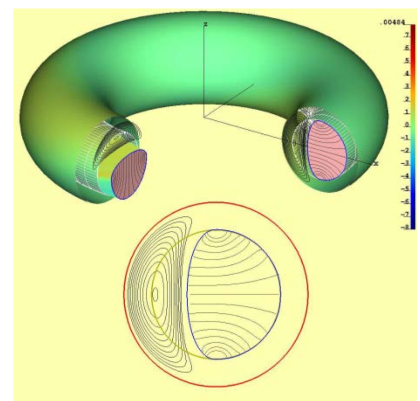

Saturation of the mode due to Hiro currents

L. Zakharov

Approximation used for M3D equilibrium

- Large-aspect-ratio torus, circular cross-section.
- In plasma ($0 \le r \le a$-δ), constant p and q provided by :

$$RB_\phi(r) = \frac{q_0^2 R_0^2 B_0}{q_0^2 R_0^2 + r^2} \qquad J_\phi(r) = \frac{2 q_0^3 R_0^3 B_0}{\left(q_0^2 R_0^2 + r^2\right)^2} \qquad p(r) = p_0$$

- In boundary layer (a-$\delta \le r \le a$) $q \rightarrow q_a$, p drops linearly:

$$RB_\phi(r) = \frac{q_0^2 R_0^2 B_0}{q_0^2 R_0^2 + (a-\delta)^2} \qquad J_\phi(r) = \frac{\gamma r}{\sqrt{\dfrac{2\gamma\left(r^3 - a^3\right)}{3} + \dfrac{a^4 B_{b,z}^2}{q_a^2 R_0^2}}} \qquad p(r) = p_0 - \gamma\left[r - (a-\delta)\right]$$

- In vacuum, p is low, J vanishes, fields are continuous:

$$RB_\phi(r) = \frac{q_0^2 R_0^2 B_0}{q_0^2 R_0^2 + (a-\delta)^2} \qquad J_\phi(r) = 0 \qquad p(r) = \varepsilon$$

- Here, q_0=B_0=1, q_a=0.75, a=0.6; the aspect ratio R_0, layer thickness δ, and pressure ratio p_0/ε are free parameters, and

$$\gamma = \frac{3}{2\left[(a-\delta)^3 - a^3\right]}\left\{\frac{q_0^2 R_0^2 B_0^2 (a-\delta)^4}{\left[q_0^2 R_0^2 + (a-\delta)^2\right]^2} - \frac{a^4 B_{b,z}^2}{q_a^2 R_0^2}\right\}, \quad p_0 = \varepsilon + \gamma\delta$$

Profiles

- R_0=72, δ/a=0.1, p_0/ε=100, n_0/n_{vac}=1 $\rightarrow$ T_0/T_{vac} = 100
- 191 radial zones

pressure

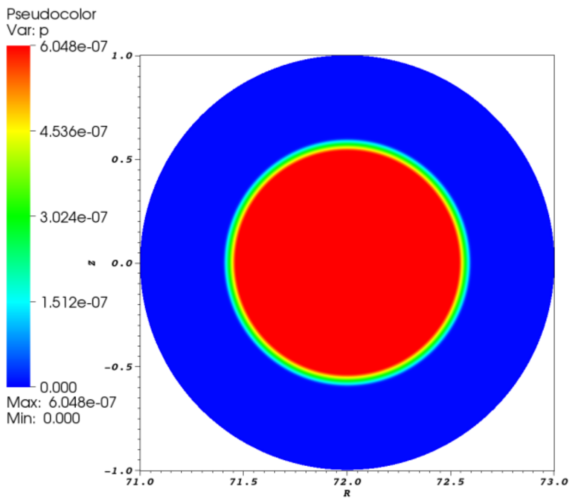

10% boundary, 190 radial, before relaxation

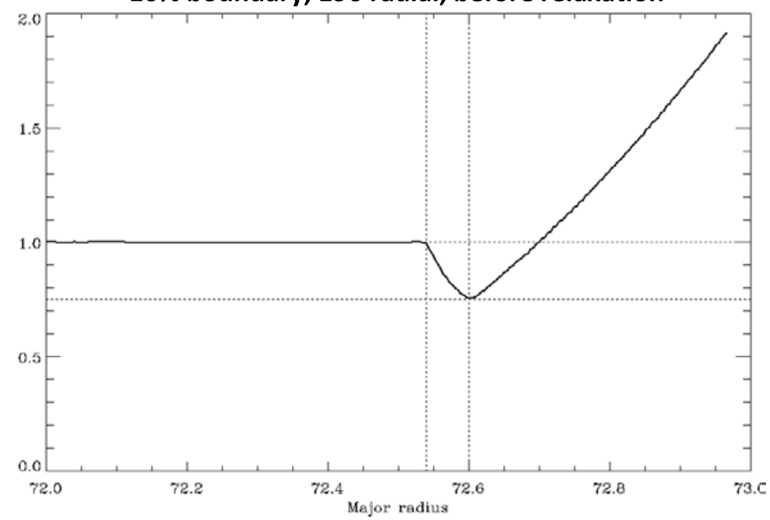

toroidal current density

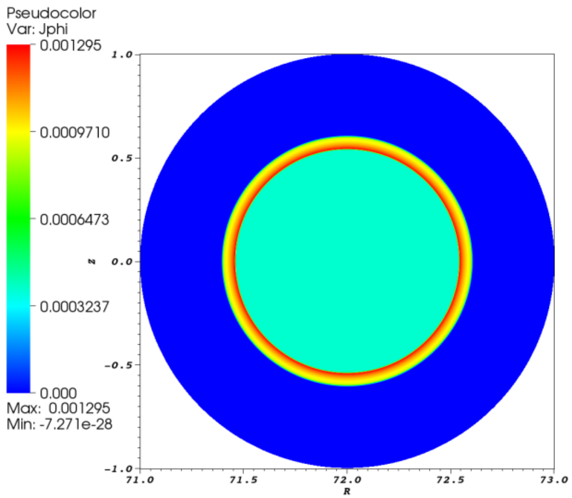

10% boundary, 190 radial, after relaxation

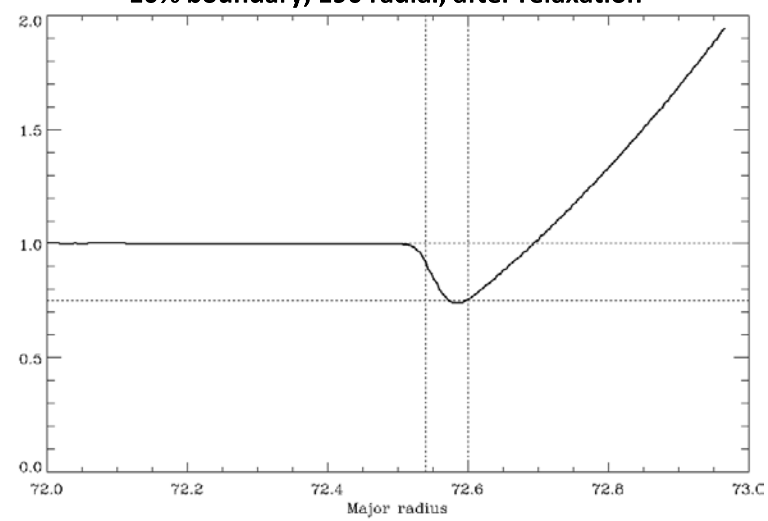

The kink perturbation

- The DSC perturbation is a small helical deformation of the plasma surface:

$$\rho \to a + \xi_{1,1} \cos(\omega - \phi)$$

- This is a rigid rightward displacement of the plasma column.

- M3D perturbs the incompressible poloidal velocity stream function to achieve the same effect:

$$U_0(r,\theta,\phi) = \begin{cases} r\xi_{1,1} \sin(\theta - \phi), & 0 \le r \le a \\ 0, & a < r \end{cases}$$

- Run linearly to find eigenmode, then use it as small initial perturbation for 3D nonlinear calculation.

Linear eigenmode calculation

n=1 eigenmode
is a 1,1 external kink

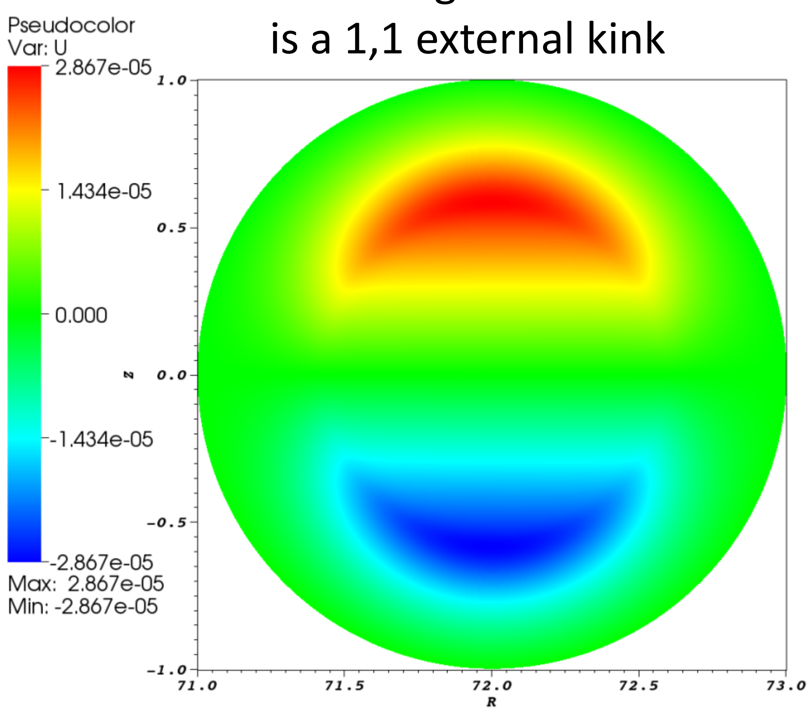

$\gamma\tau_A = 0.00583$

current and flow patterns

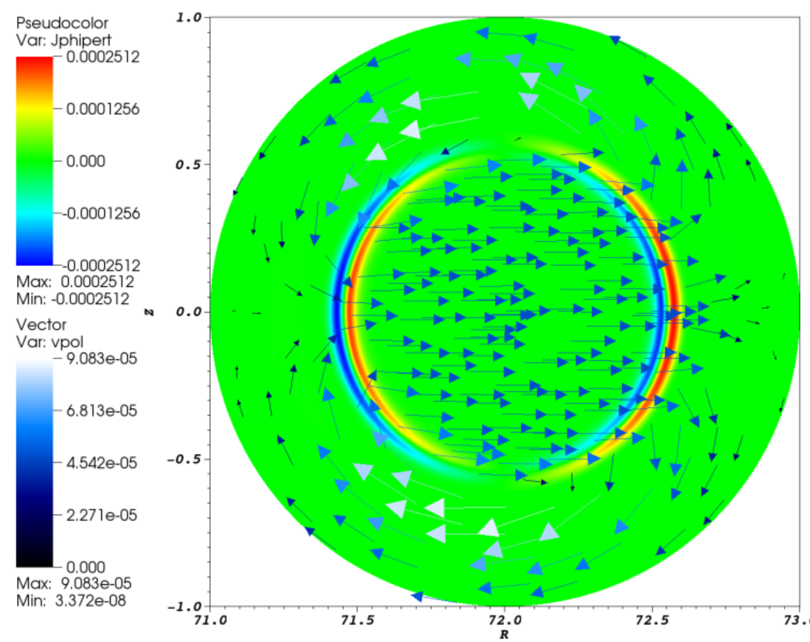

Details:

$\eta_{plas} = 10^{-6}$; $\eta_{vac} \approx 9.5 \times 10^{-4}$; $\eta_{\mathrm{wall}} = 0$
$\mu = 10^{-5}$; $\mu_{\mathrm{H\_tor}} = 0$
$\kappa_\perp = 10^{-6}$; $\kappa_{||} = 500$
density evolution off

- Rigid displacement of plasma column
- Rearrangement of "vacuum" to avoid compression
- 1,1 toroidal current sheets of both signs at plasma boundary

3D nonlinear behavior, ideal wall only (FBK)

Details:
$\eta_{plas} = 10^{-6}$; $\eta_{vac} \approx 9.5 \times 10^{-4}$; $\eta_{wall} = 0$
$\mu = 10^{-5}$; $\mu_{H\_tor} = 10^{-3}$
$\kappa_{\perp} = 10^{-6}$; $\kappa_{||} = 5 \times 10^{2}$

initial pert.: n=1 only
density evolution off
ohmic heating on
$0 \leq n \leq 20$ (64 planes)

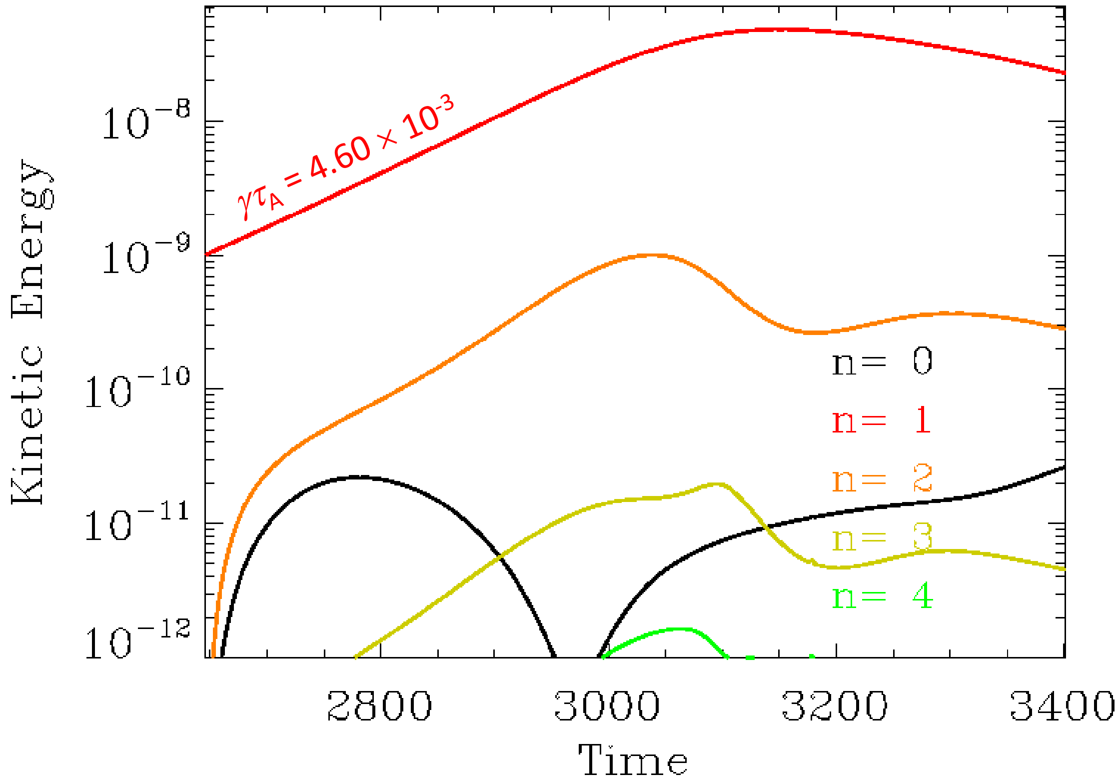

n=1 KE saturates at 4.804×10^{-8}
in 504 Alfvén times.

Snapshots of FBK

	t = 2700	t = 2900	t = 3000	t = 3100	t = 3400
Resistivity	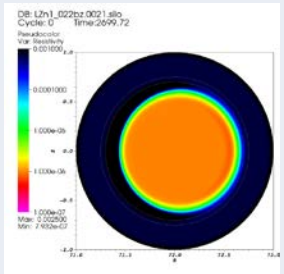	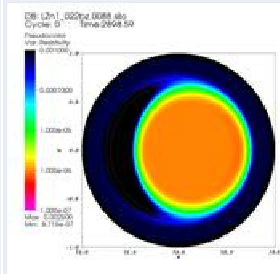	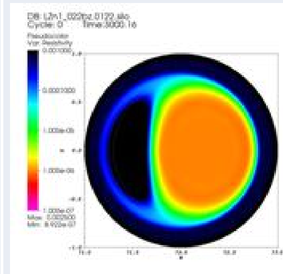	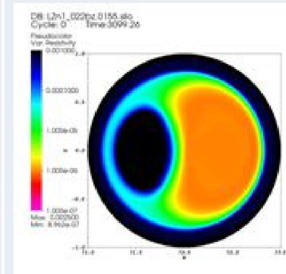	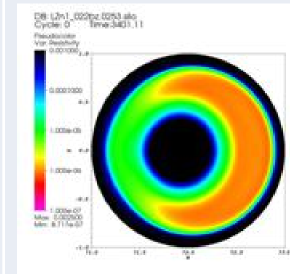
Net J_φ	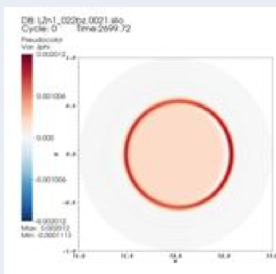	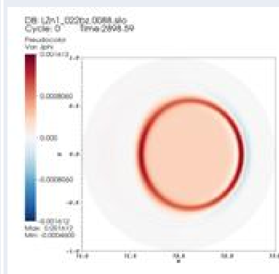	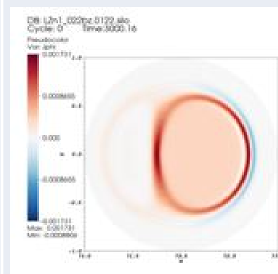	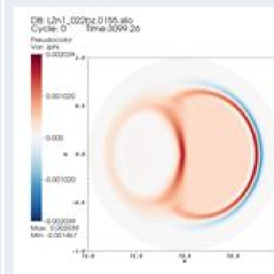	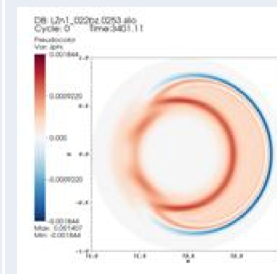
Perturbed J_φ	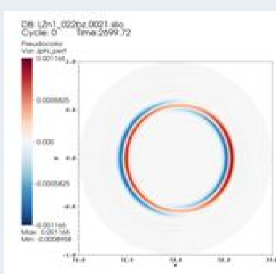	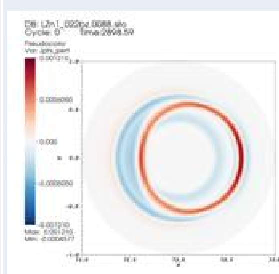	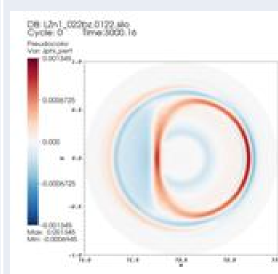	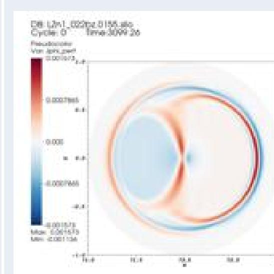	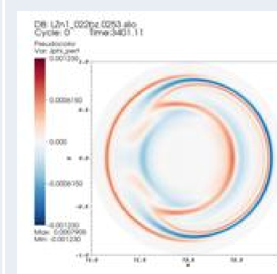

Segmented Tile Model

- Tiles are modeled as an annular region inside the computational domain from r=0.7 to r=0.7+δ.
- When not wetted, tiles behave as ordinary vacuum/plasma ($\eta \propto T^{-3/2}$).
- For wetted region of tile surface (0.7 < r < 0.7+δ **AND** $p > [p_{max} + 3p_{min}]/4$), we set $\eta \equiv \eta_{tile} \leq \eta_{plasma}$.
- Outer boundary of annulus is cold ($T = \varepsilon$ for $r > 0.7+\delta$), chills plasma when in thermal contact.
- No special conditions are imposed on velocity or force balance in tile region.

3D Nonlinear behavior with tile surface at 0.7<r<0.75, only wetted part conducting, outer edge cold, $0 \leq n \leq 9$ (WTK)

Approx. plasma boundary vs. time

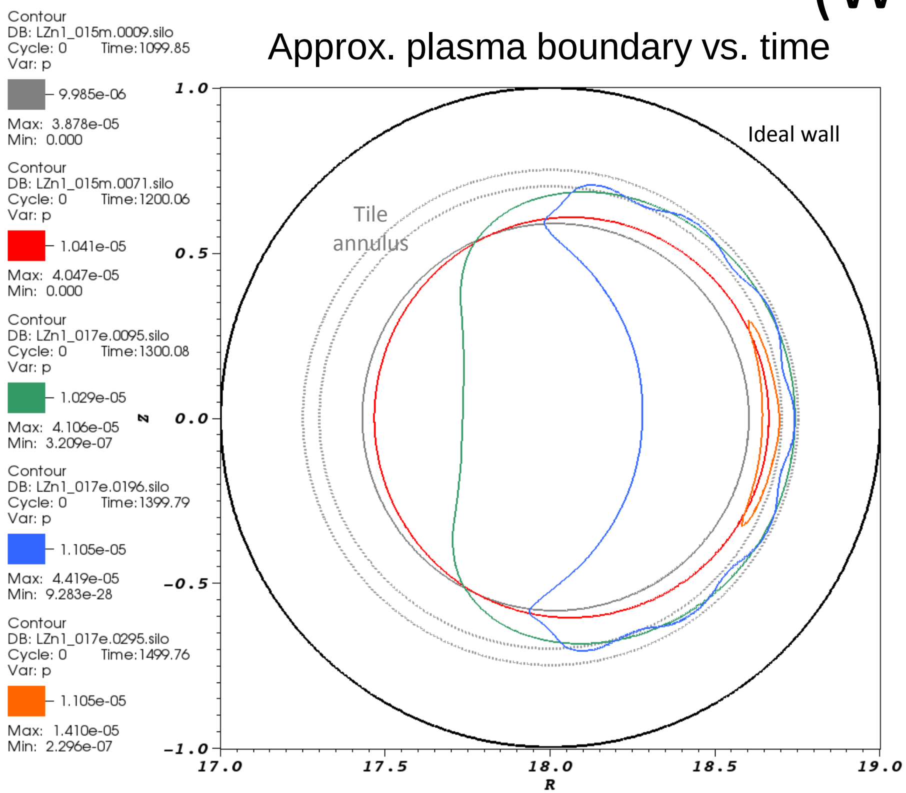

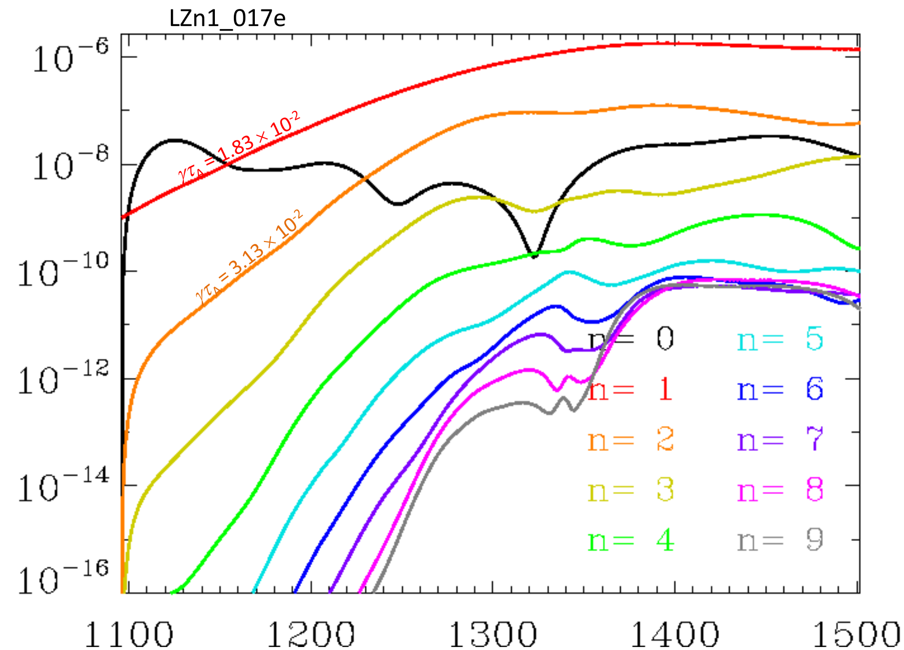

<u>Details</u>:

η_{plas} = 10^{-6}; $\eta_{vac} \approx 9.5 \times 10^{-4}$; $\eta_{\mathrm{wall}} = 0$; $\eta_{tile} \approx 10^{-7}$

$\mu = 10^{-5}$; $\mu_{\mathrm{H\_tor}} = 10^{-3}$

$\kappa_{\perp} = 10^{-6}$; $\kappa_{||} = 5 \times 10^{2}$

density evolution off

ohmic heating on

Saturates in 300 Alfvén times, develops higher-*m* corrugations, then annihilates on tile surface.

Snapshots of WTK

	Resistivity	Net J_φ	Perturbed J_φ	Wetted region	Net J_φ on tiles
***t* = 1204**	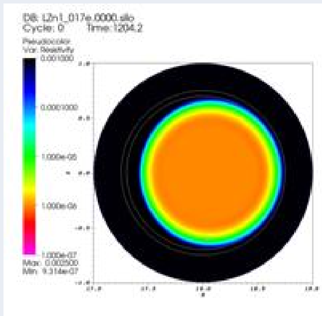	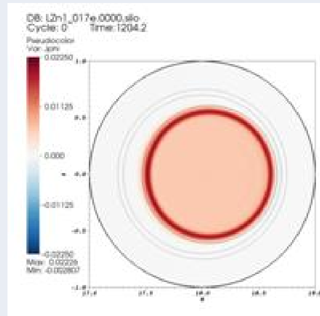	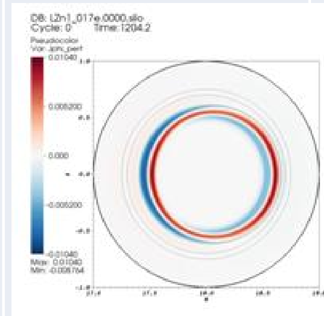	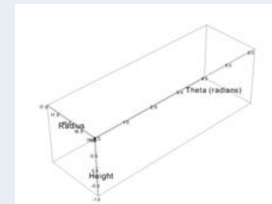	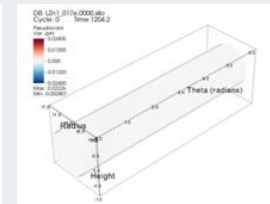
***t* = 1300**	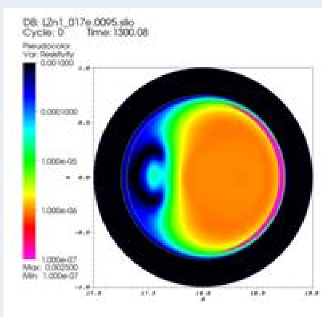	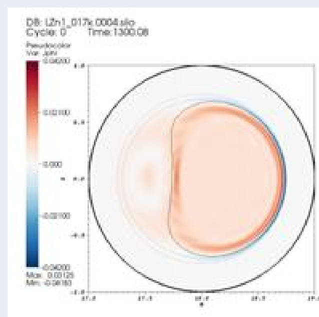	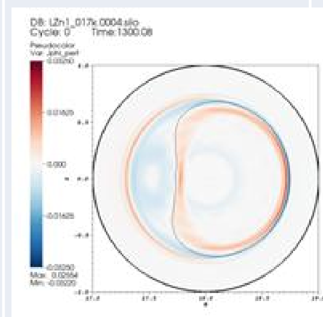	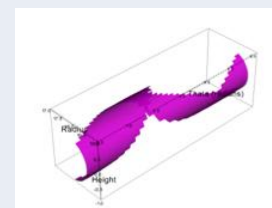	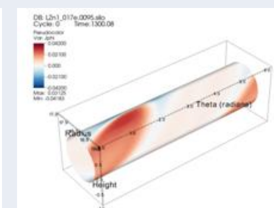
***t* = 1400**	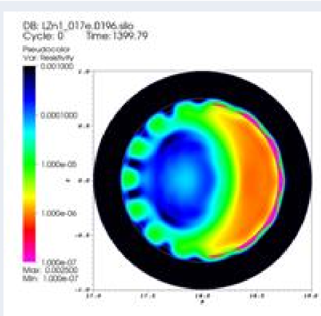	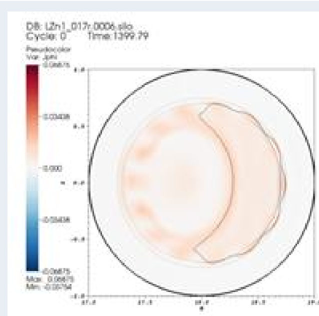	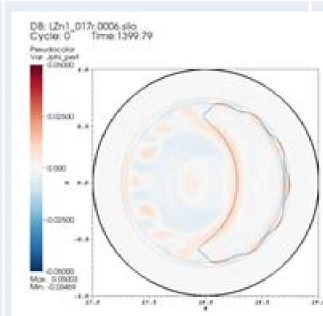	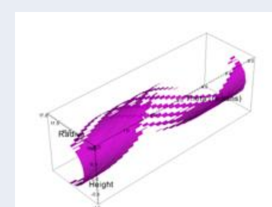	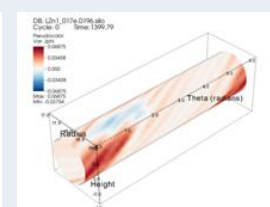

Summary of verification results

- The M3D code can represent a reasonable facsimile of the ideal straight-cylinder equilibrium with surface current.

- M3D sees more complex behavior than the idealized saturated kink solution, namely unstable modes with $n>1$ and the formation of a vacuum bubble.

- The interaction of the plasma surface currents with the ideal wall in the free boundary kink case is in line with the DSC result.

- In the wall-touching kink case, tile currents interact with the plasma surface ("Hiro") current to slow plasma motion, as in the DSC result. As in DSC, the plasma retains finite velocity normal to the tile surface, and can penetrate it on a time scale longer than that of the ideal kink.

Outline

- Verification of M3D with the DSC test problem
  - Equilibrium & stability
  - Nonlinear saturation of free boundary kink
  - Nonlinear saturation of wall-touching kink
- NSTX VDE study
  - Experimental observations
  - M3D results
  - IVB results
- Conclusions

NSTX XP833 (2010):

Halo current dependencies on I_p/q_{95}, vertical velocity, and halo resistance

Reference shot without forced disruption drive, based on 129416:

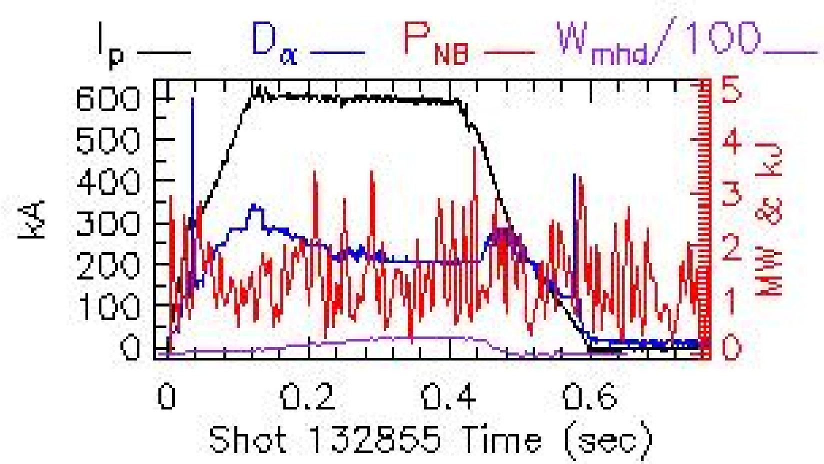

Shot 132859, with deliberately misadjusted vertical field control, terminates in VDE:

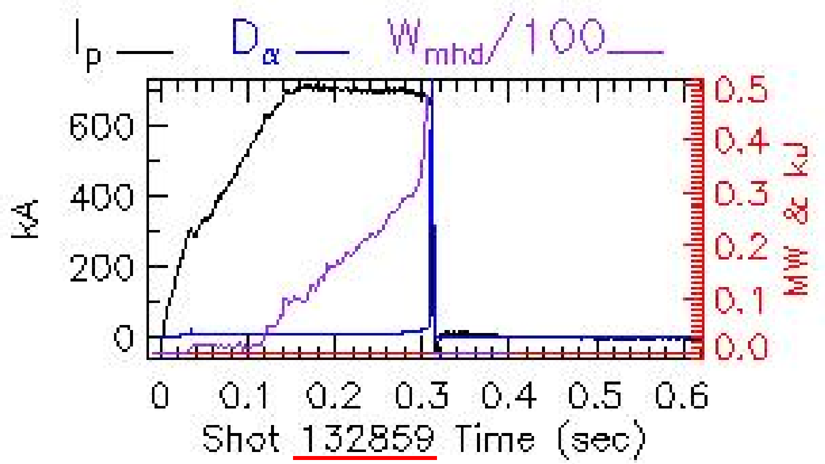

S. Gerhardt

Layout of NSTX halo current diagnostics

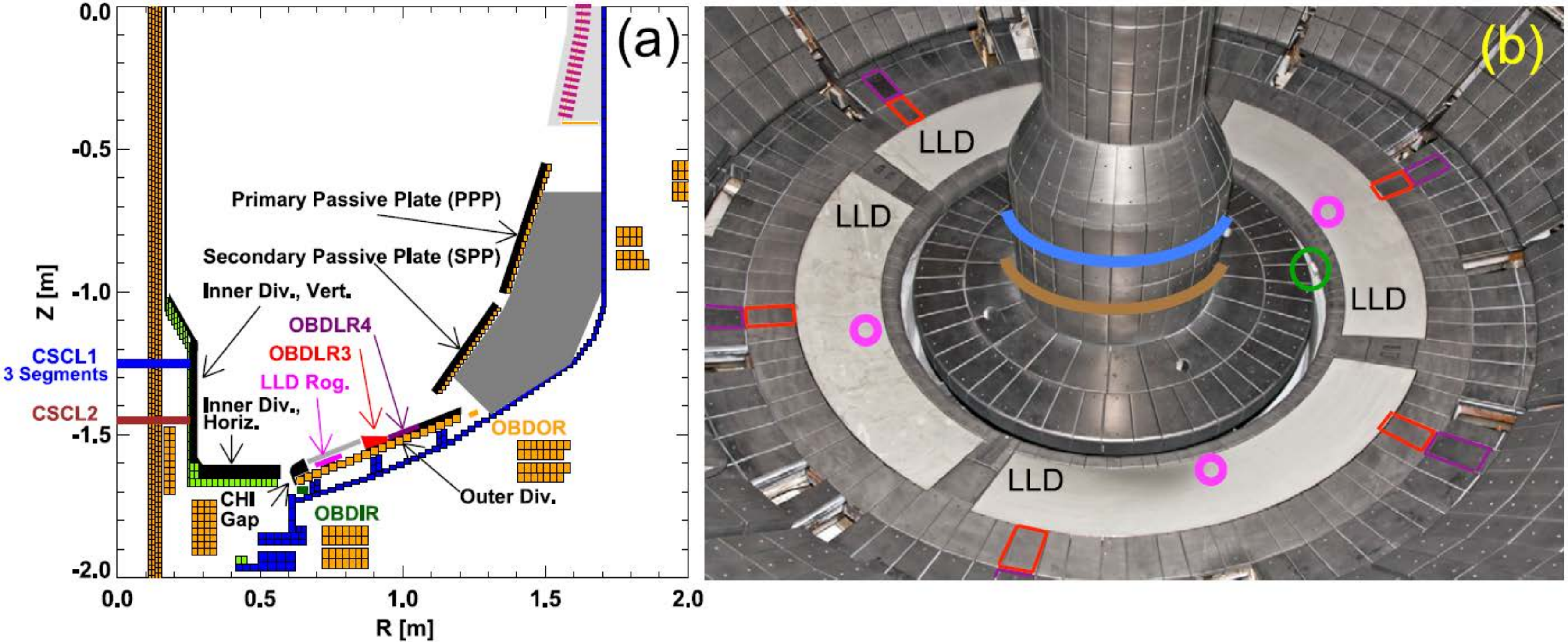

Halo current is inferred from transient TF measurements under several divertor tiles and plates at about six toroidal locations. Transient vessel forces are not measured.

Figure reproduced from S.P. Gerhardt, J. Menard, S. Sabbagh and F. Scotti, *Nucl. Fusion* **52** (2012).

Strongly Non-Axisymmetric Halo Currents Detected in the NSTX Lower Divertor

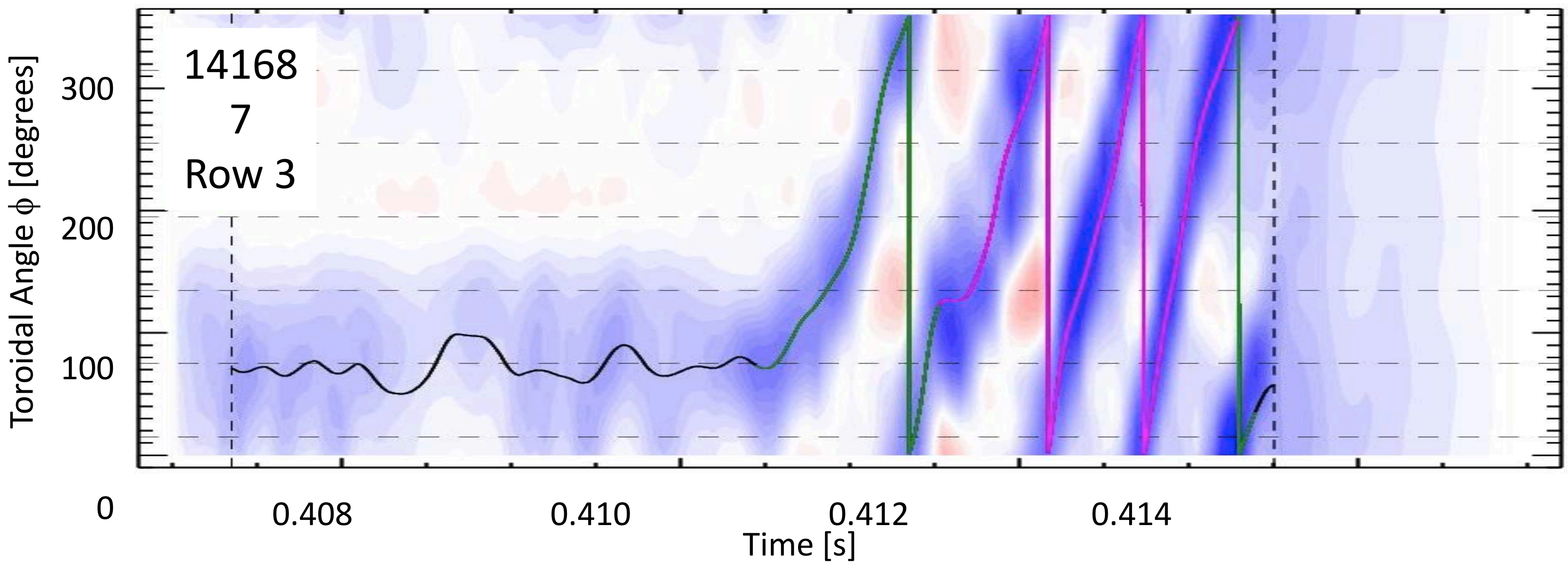

- Infer strong toroidal asymmetry, often with significant rotation, at locations where currents enter the divertor floor.

<u>Key Observations</u>

Dominant structure is typically a toroidally-rotating lobe.
Rotation is typically in the counter-direction, except for short bursts.

S. Gerhardt

Meshing the NSTX Vessel for Simulation

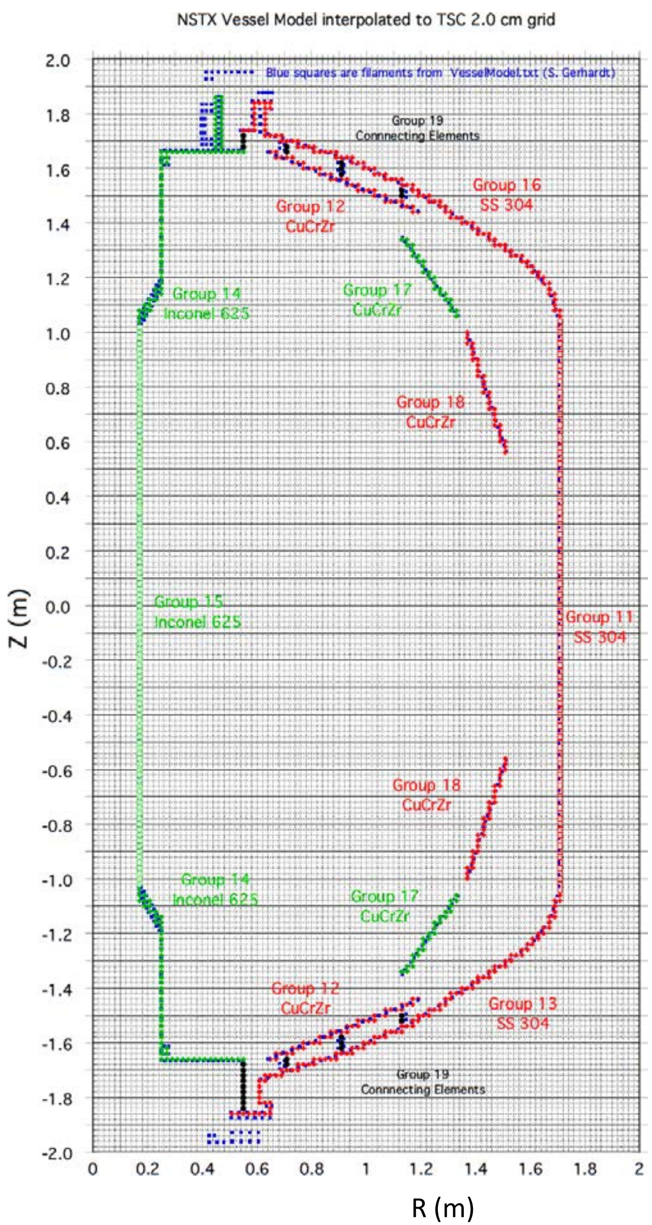

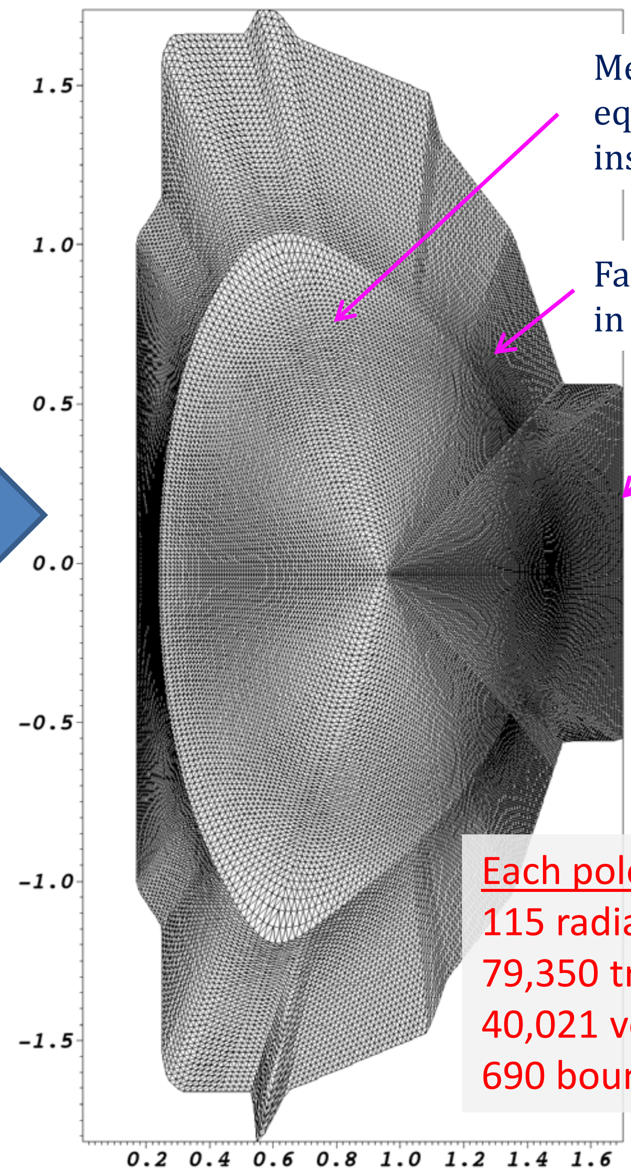

Each poloidal section has up to
115 radial zones
79,350 triangular elements
40,021 vertices
690 boundary vertices

n=1 eigenmode

η_0	5×10^{-8}
η_{vac}	1.67×10^{-4}
η_{wall}	0
μ_0	5×10^{-7}
μ_{edge}	10^{-4}
$\kappa_\perp$	10^{-5}
$\kappa_{\|\|}$	10^{-1}

Predominantly 1,1 mode at q=1 surface.

$\gamma \approx 6.5 \times 10^{-2}$

Perturbed pressure

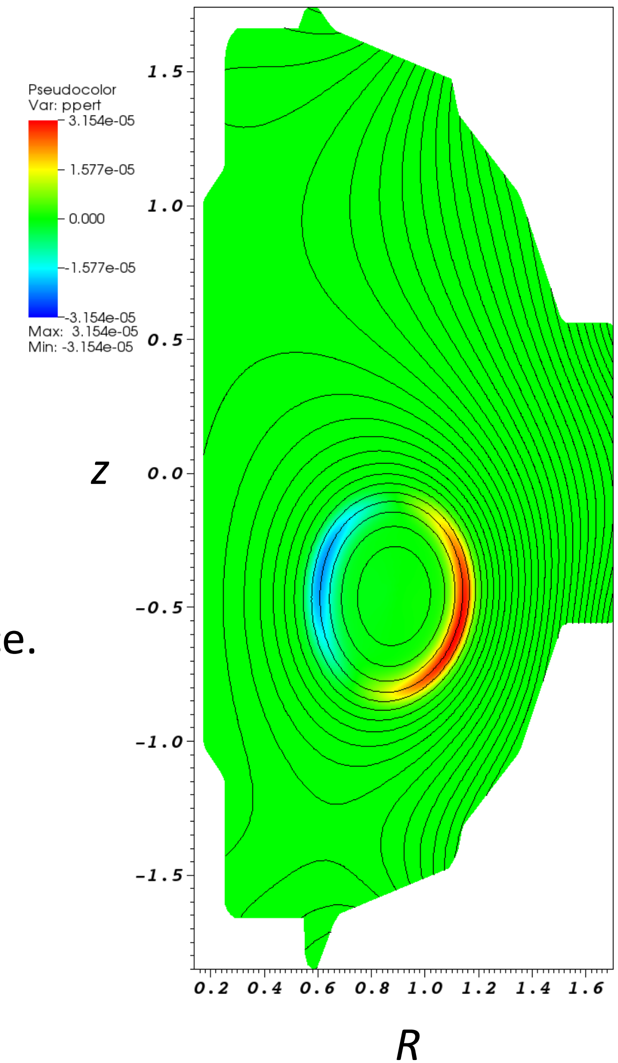

Perturbed current

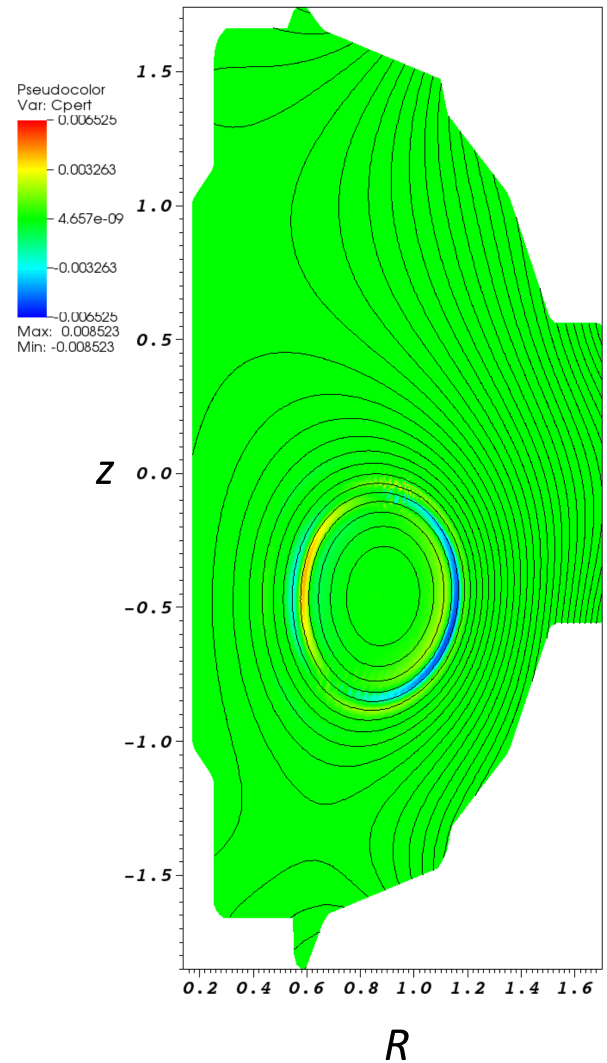

Time History (nonlinear 3D phase)

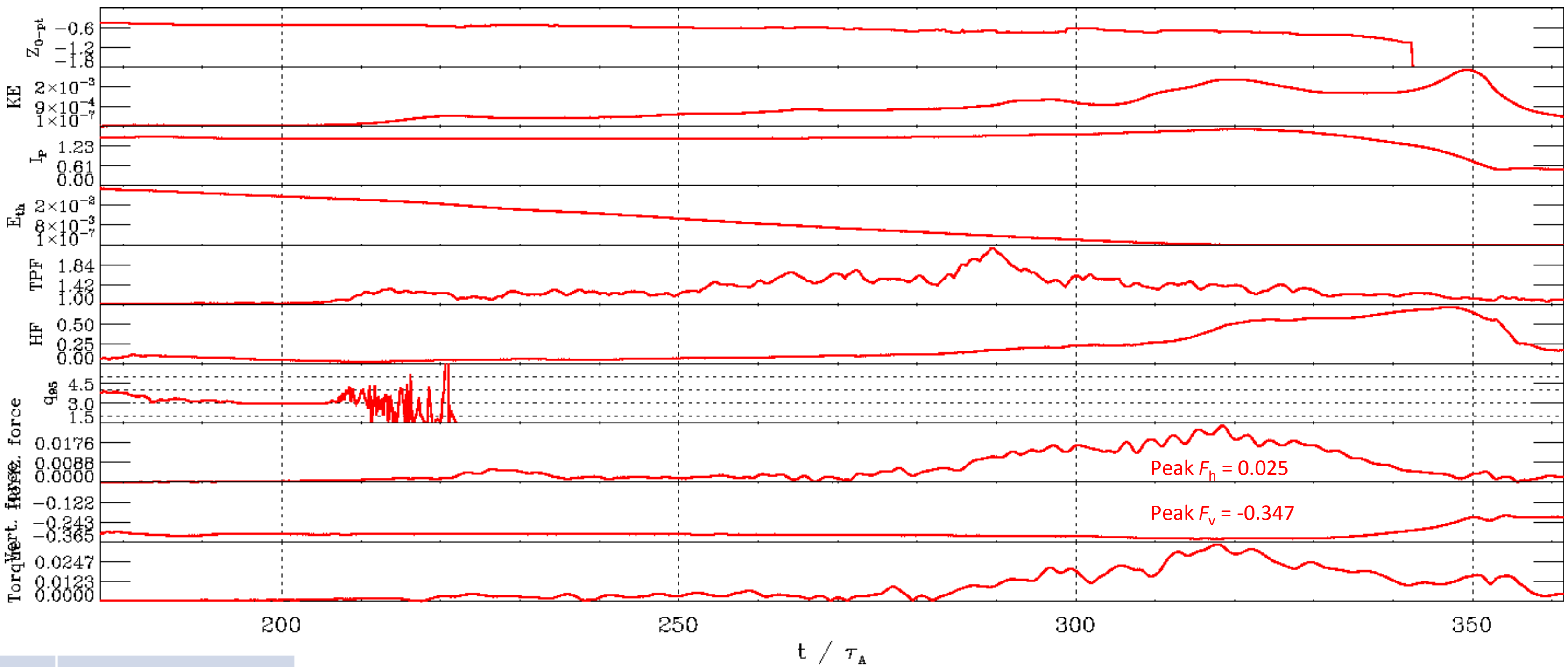

η_0	5×10^{-8}
η_{vac}	1.67×10^{-4}
η_{wall}	10^{-4}
μ_0	5×10^{-7}
μ_{edge}	10^{-4}
$\kappa_\perp$	10^{-5}
$\kappa_{\|\|}$	10^{-1}

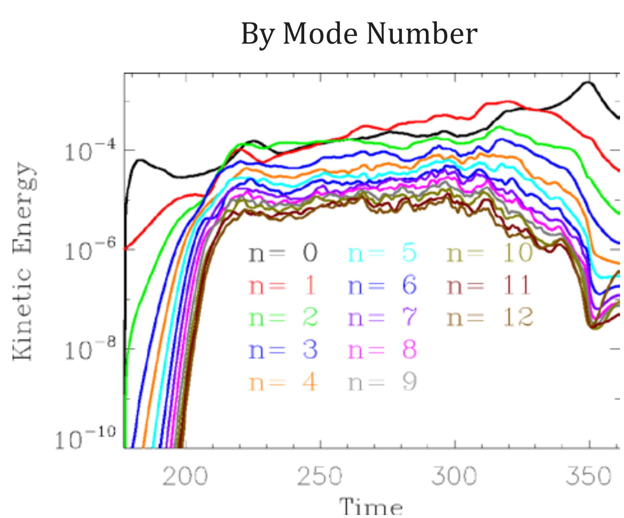

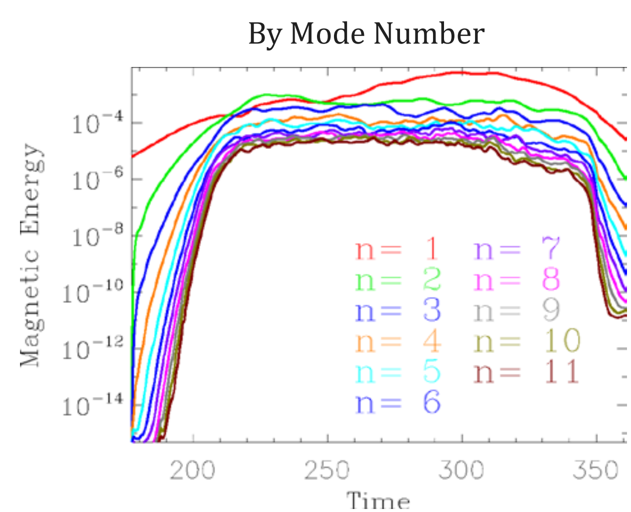

Snapshots of Nonlinear Evolution

t = 177.14

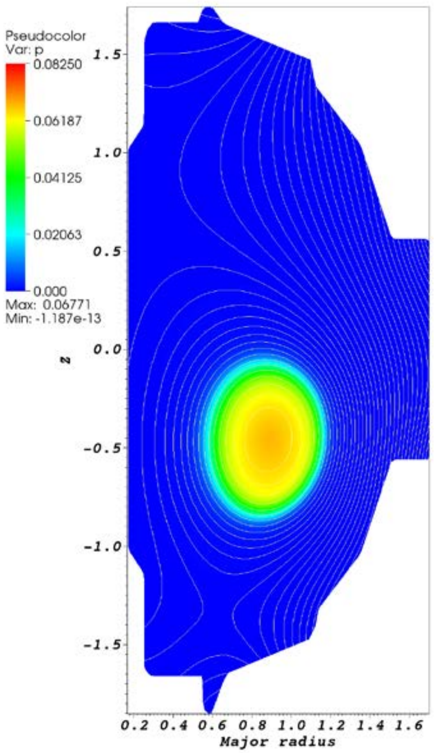

Ideally unstable displaced plasma

t = 222.99

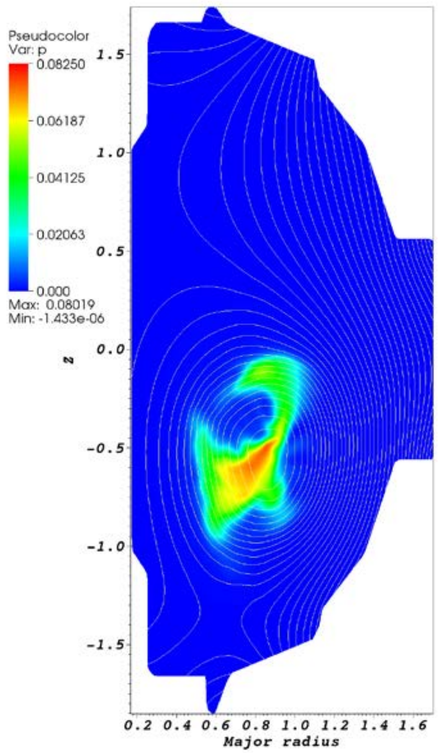

Instability couples many toroidal & poloidal modes…

t = 284.15

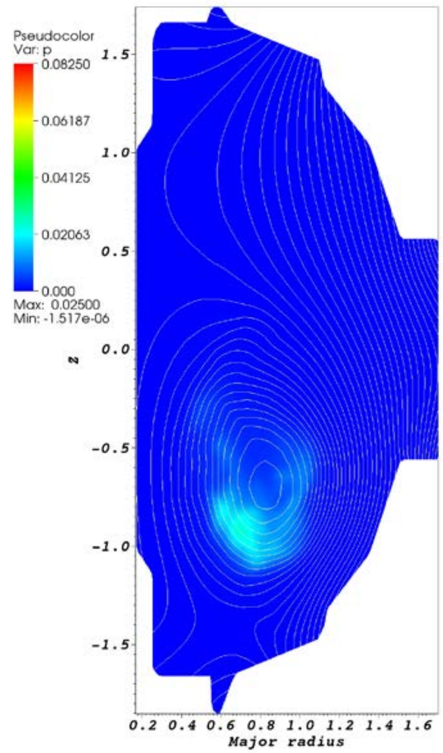

…leading to rapid thermal quench.

t = 361.49

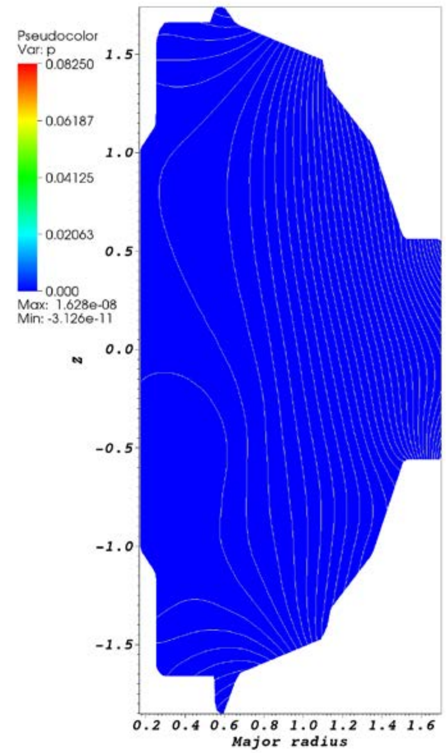

Current quench follows.

Halo Current Distribution at Peak

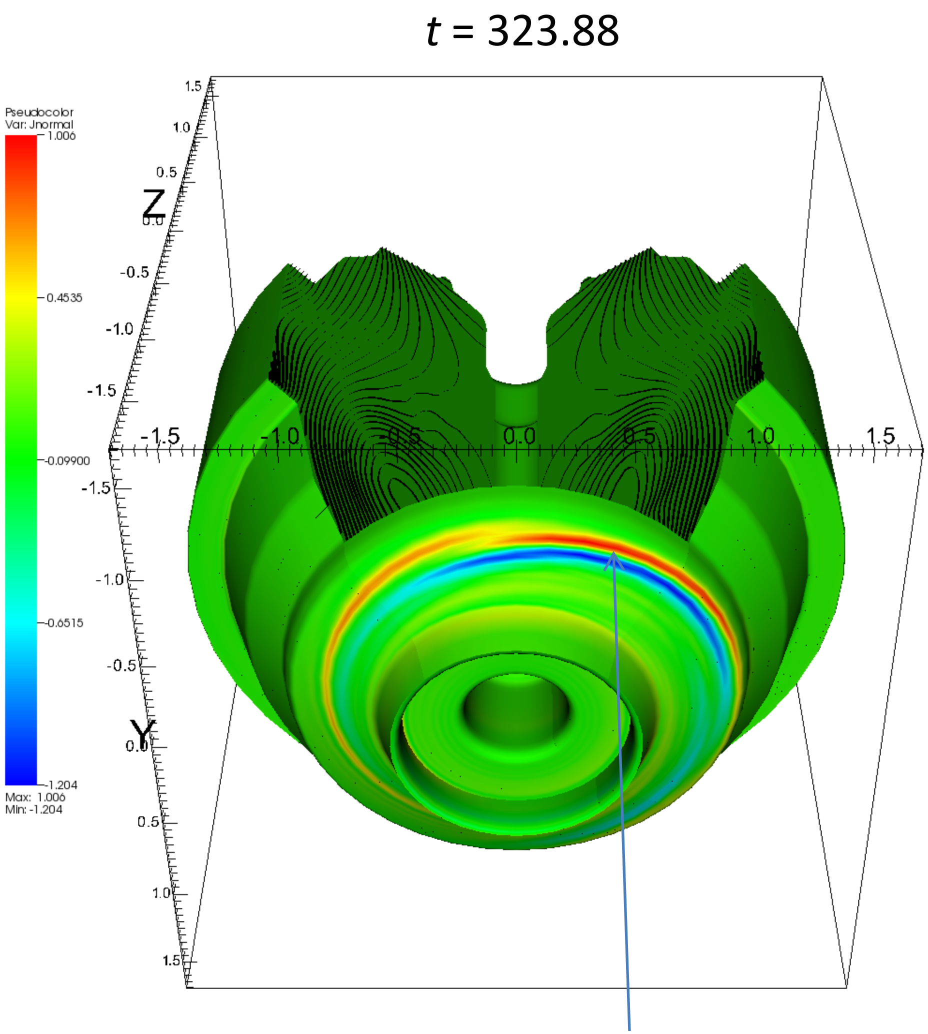

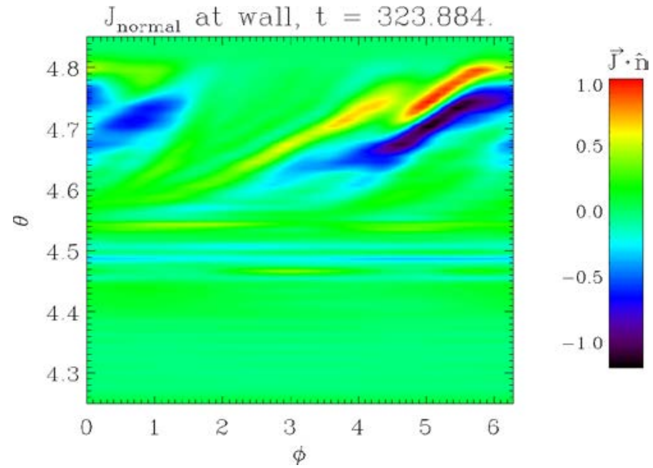

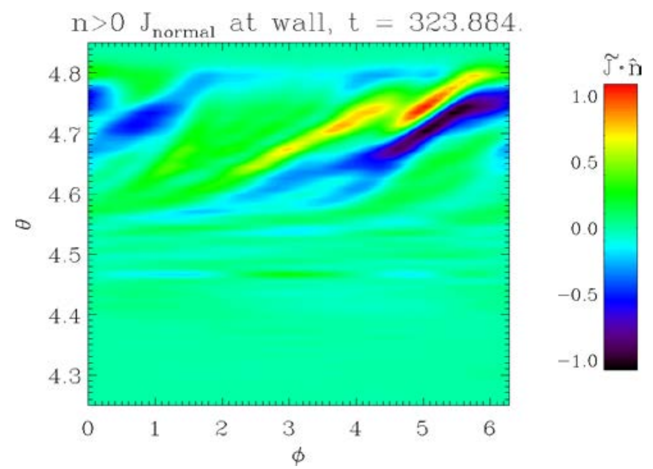

Current peaks on lower Group 12 plate.

n=1 component strongly dominates over n=0.

Halo Current Distribution vs. Time

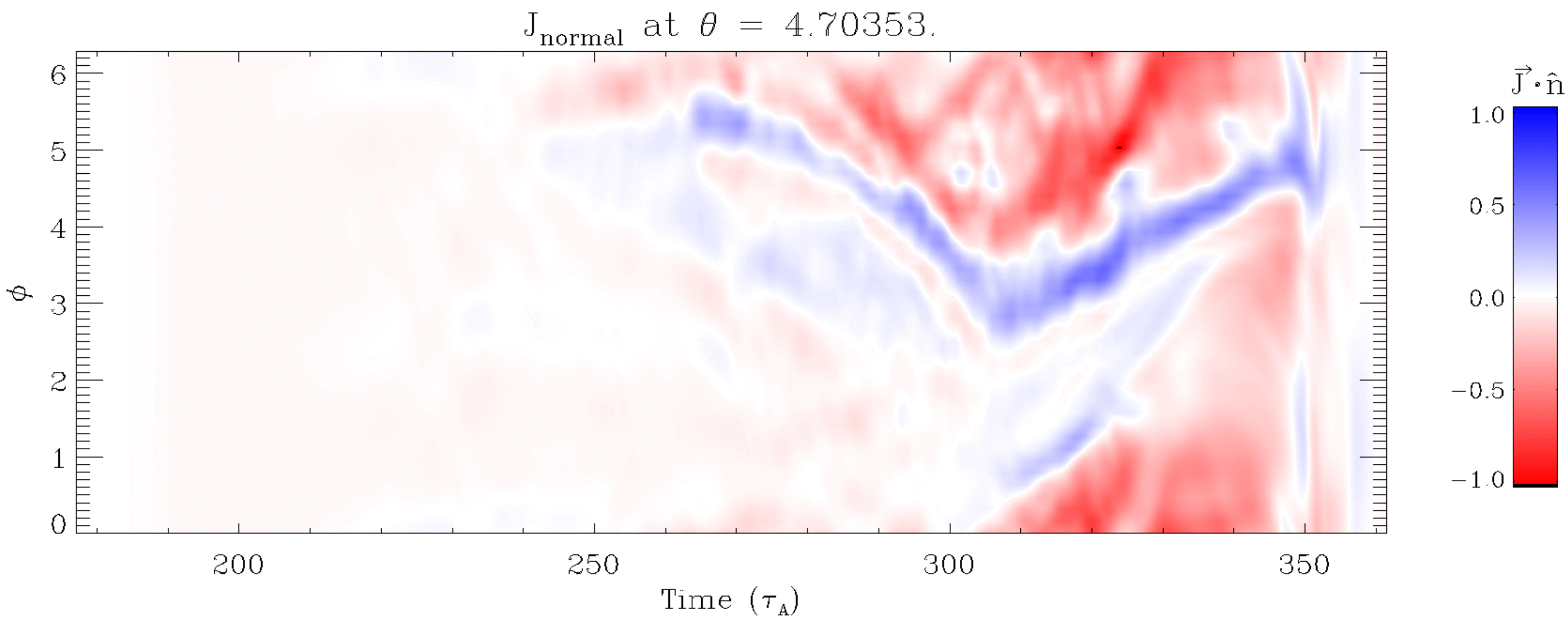

Coupling to IVB

- To assess plausibility, self-consistency of halo current results.

- Current-voltage branch code developed by J. Bialek to explore halo current distributions in vessel components.
  - User supplies exterior d**B**/dt, J_{normal}, and reference nodal voltages.
  - IVB solves for time-dependent current and voltage in arbitrary conducting structures composed of 1D, 2D, and 3D elements.

- M3D simulation data selected from two representative time slices.
  - Frame 132, t = 205.07: linear phase of instability; halo currents still axisymmetric.
  - Frame 676, t = 323.88: peak KE & current, high HF, peaking factor.

- J_{normal} on axisymmetric shell interpolated onto 2D and 3D engineering models; plasma current distribution ignored for first pass.

Axisymmetric IVB Model

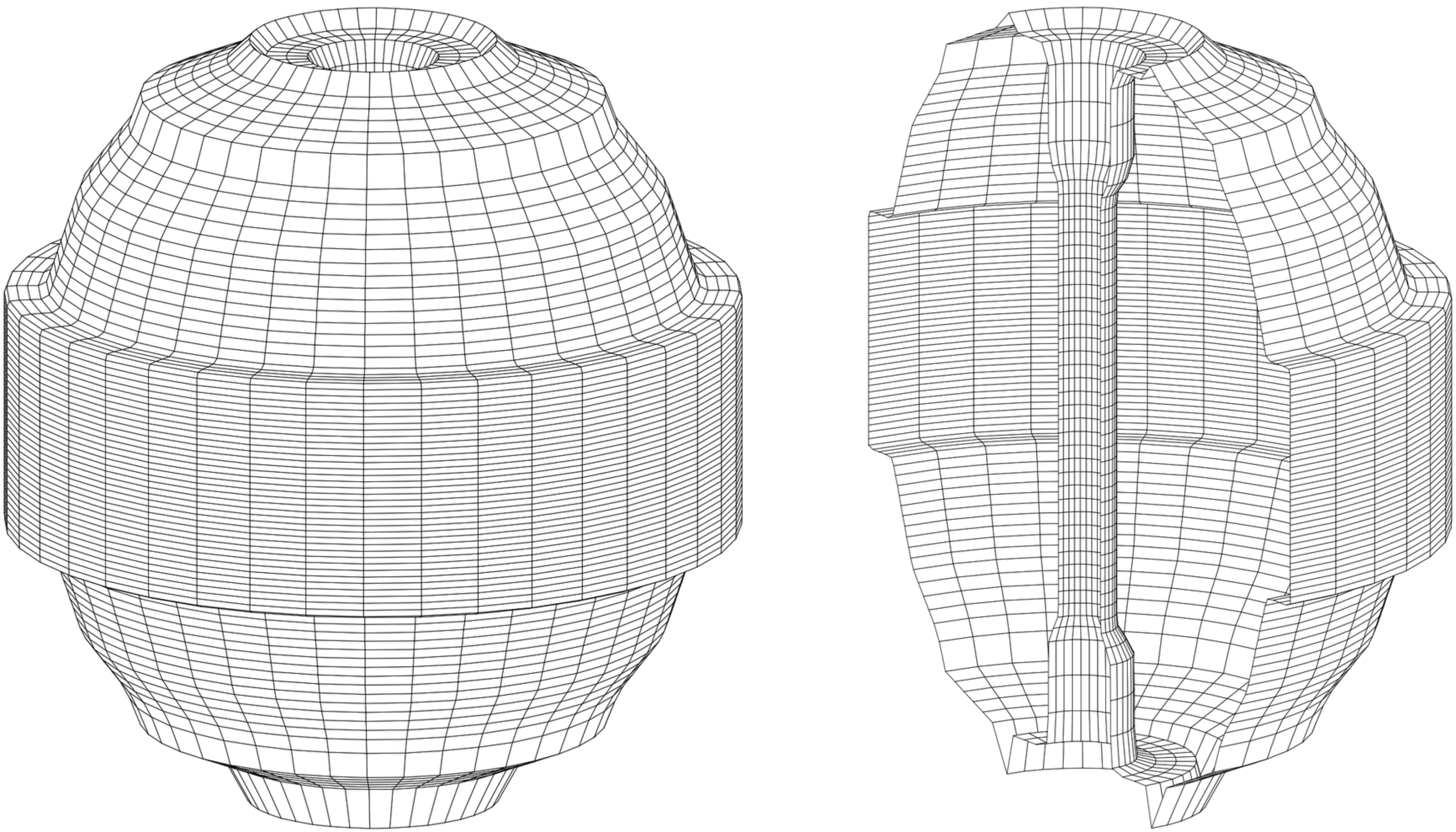

Conforms to M3D boundary.

Frame 132 current distribution

Cutaway view

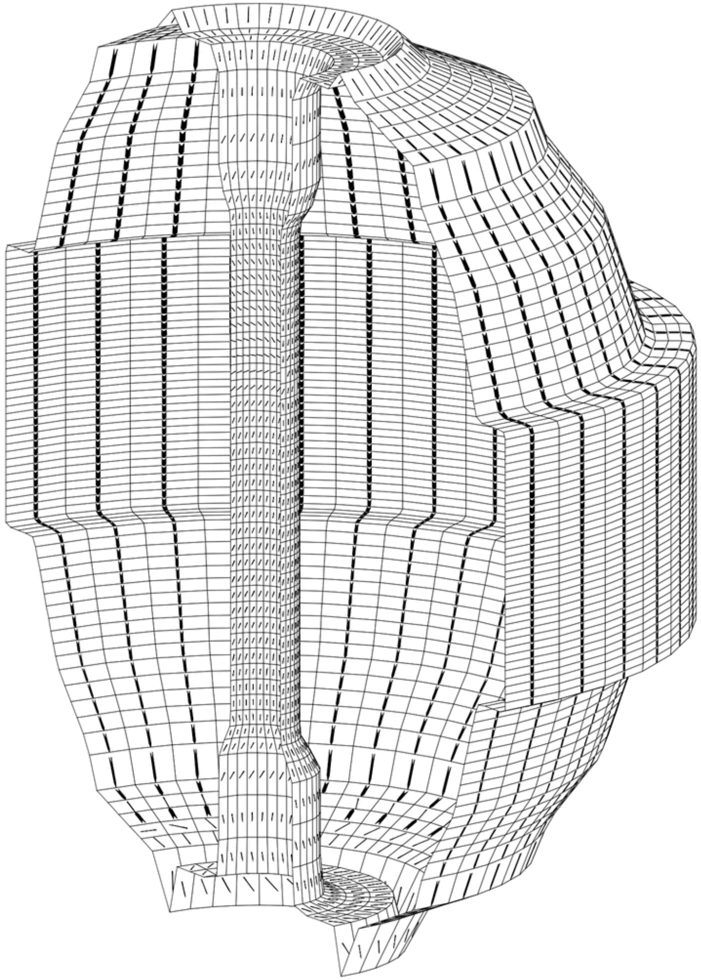

Arrow scale: surface current density up to 12 kA/m

Bottom view

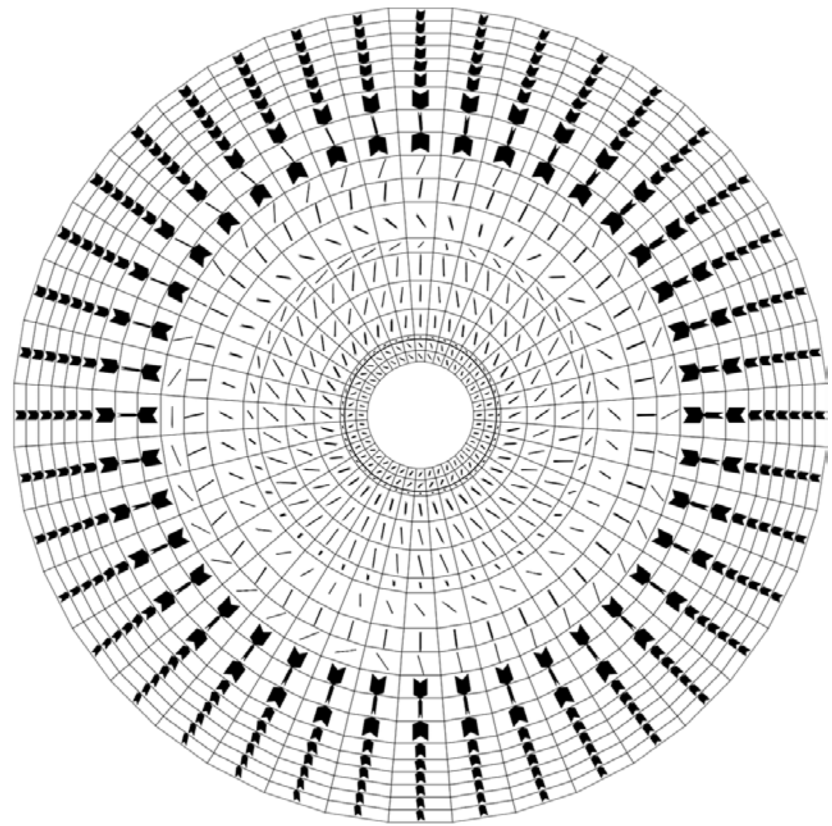

Arrow scale: surface current density up to 3.5 kA/m

Frame 676 current distribution

Cutaway view

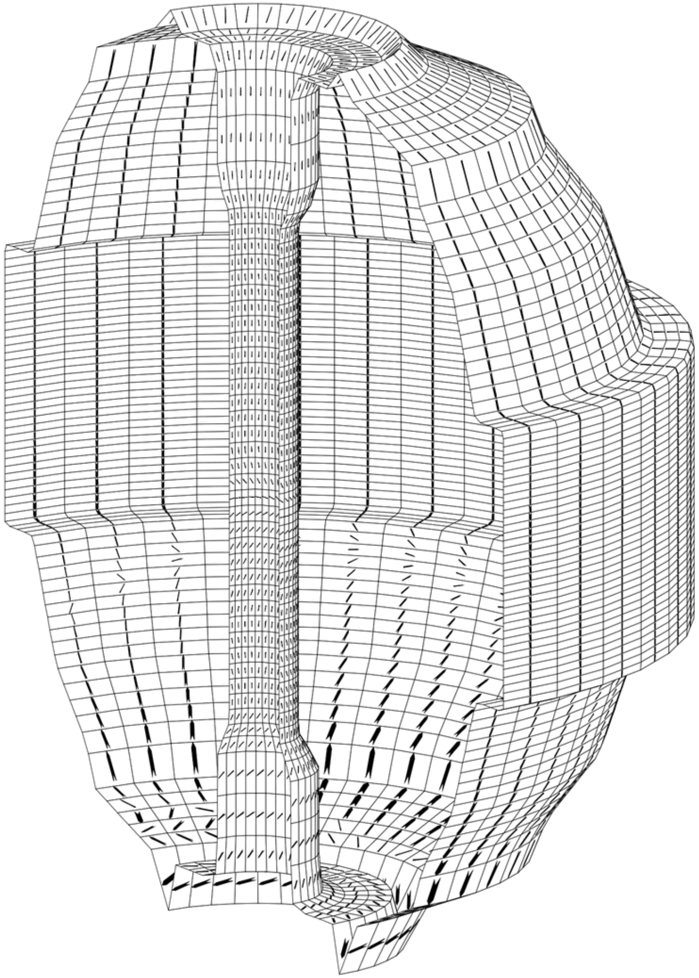

Arrow scale: surface current density up to 142 kA/m

Bottom view

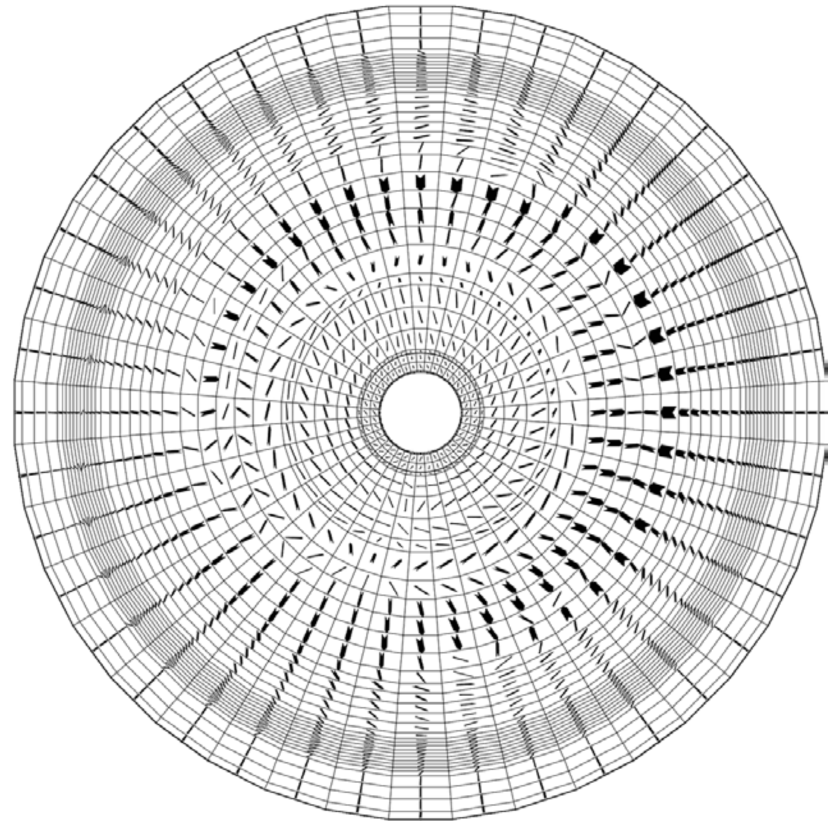

Arrow scale: surface current density up to 172 kA/m

3D IVB Model

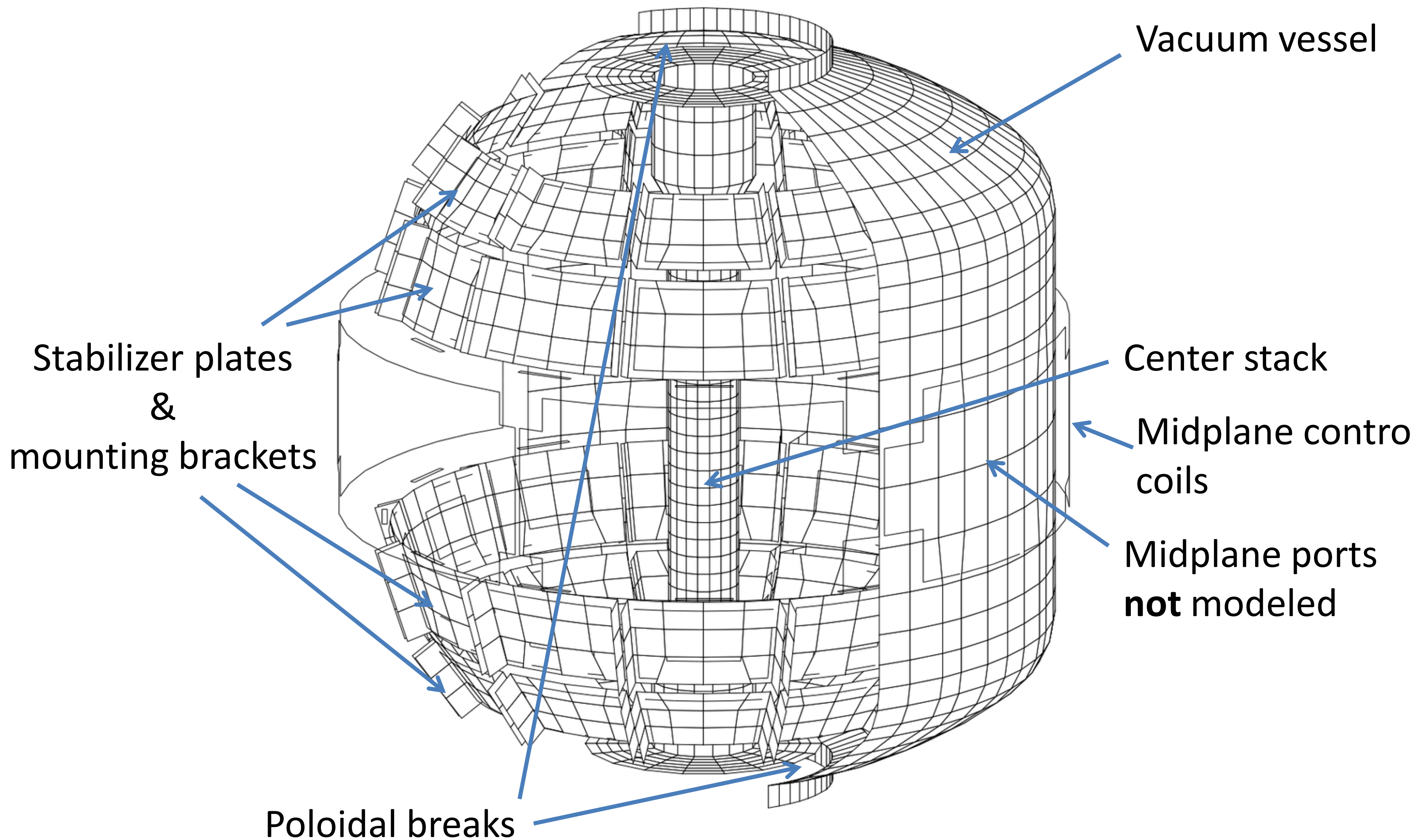

Four ground points via CHI busbar system

Mapping frame 132 J_{normal} onto 3D model

Cutaway view

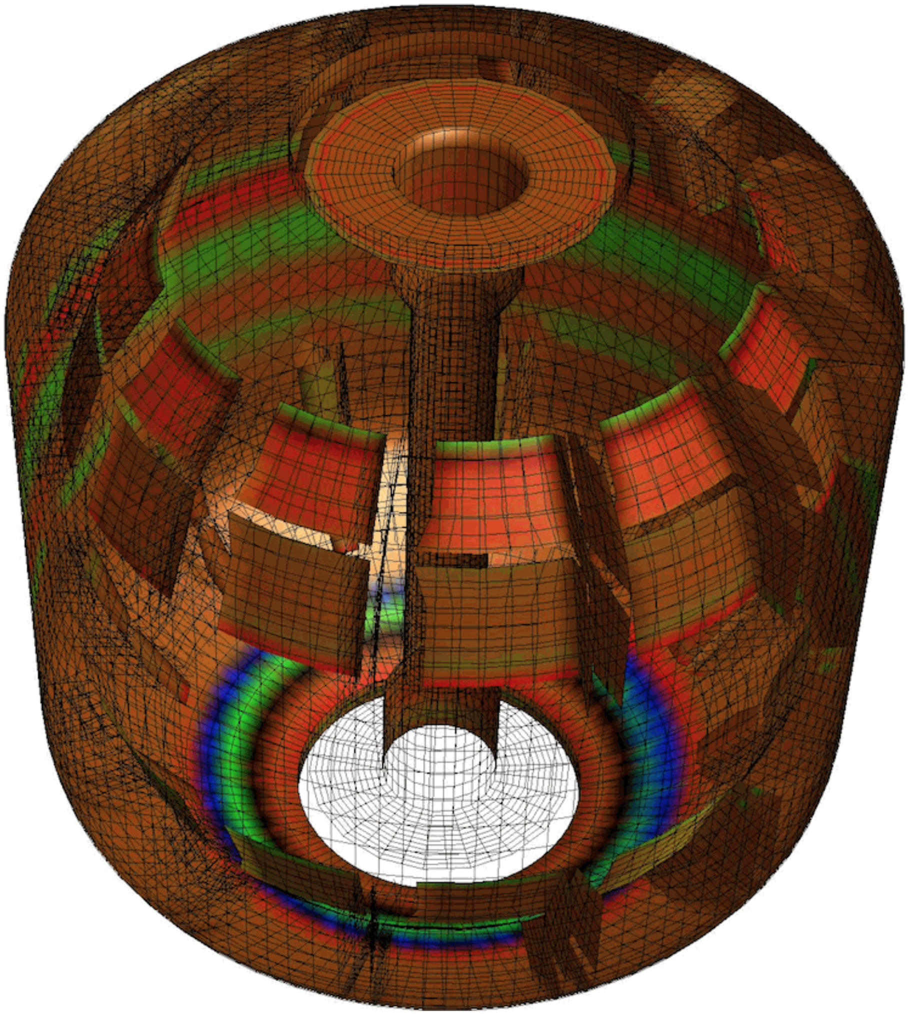

Bottom view

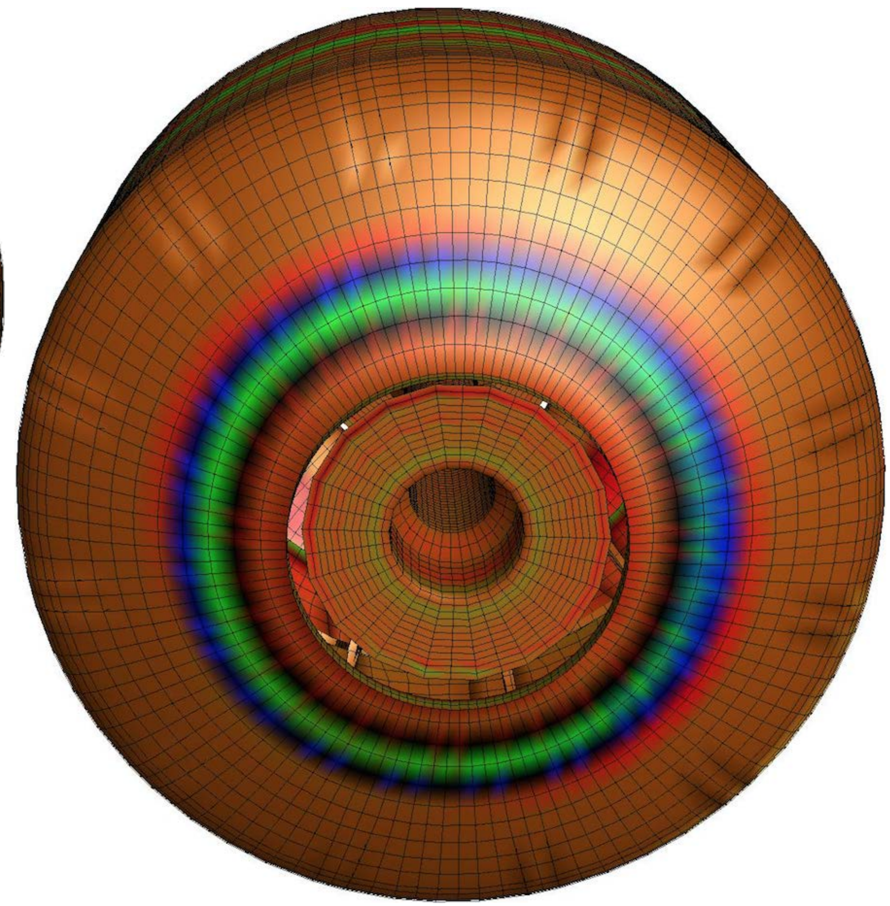

Frame 132 current distribution

Cutaway view

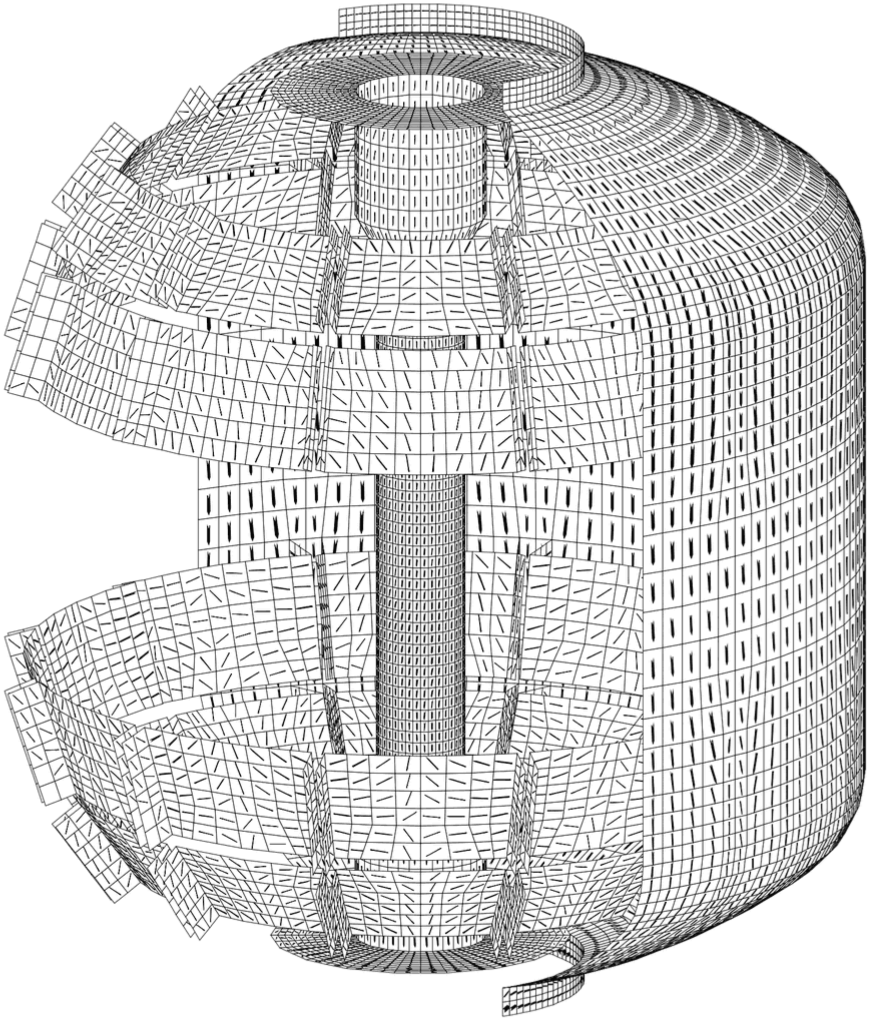

Arrow scale: surface current density up to 6 kA/m

Exterior view

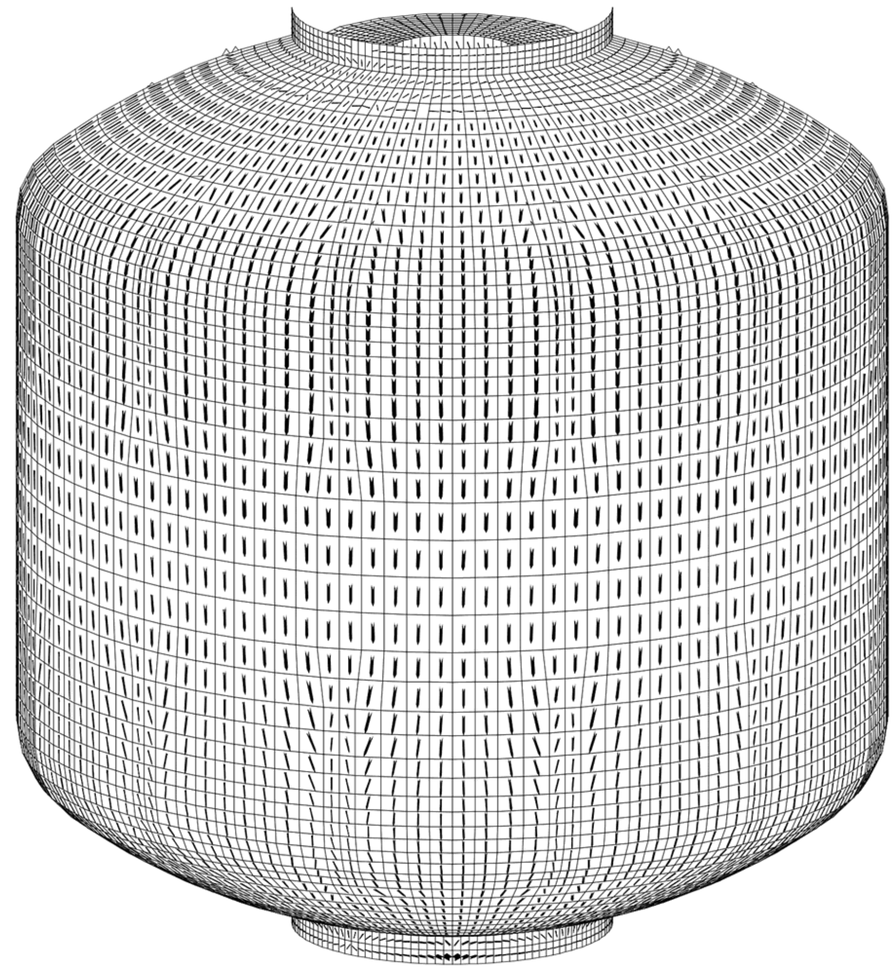

Arrow scale: surface current density up to 6 kA/m

Mapping frame 676 J_{normal} onto 3D model

Cutaway view

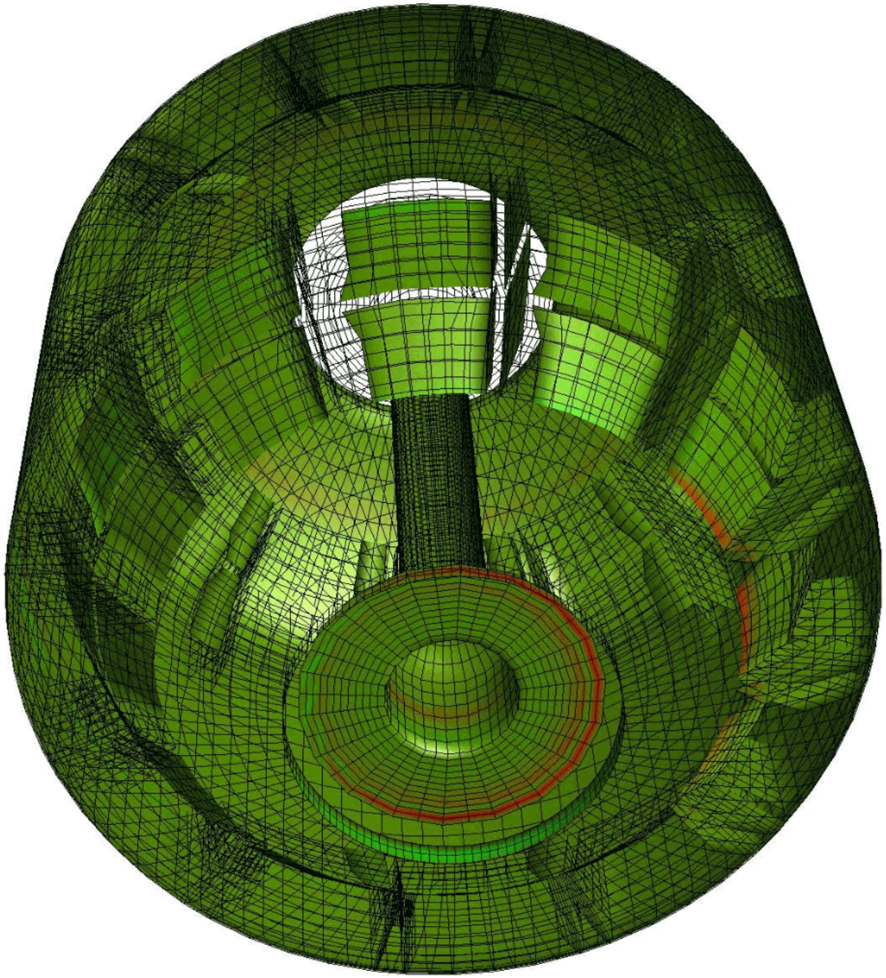

Bottom view

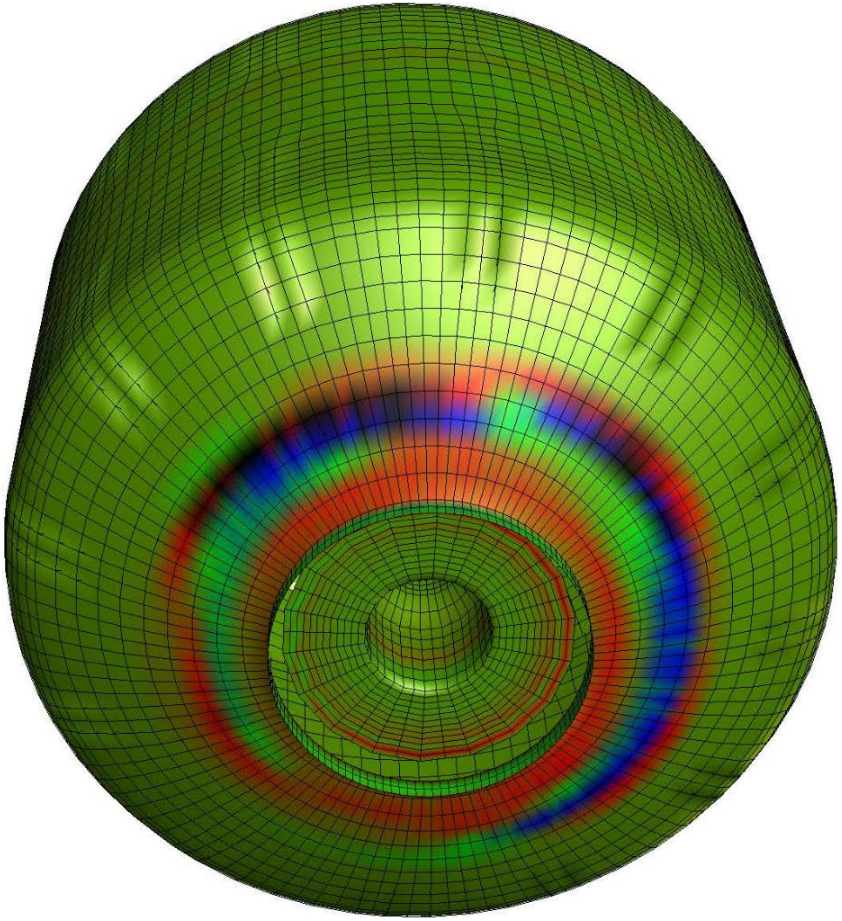

Frame 676 current distribution

Cutaway view

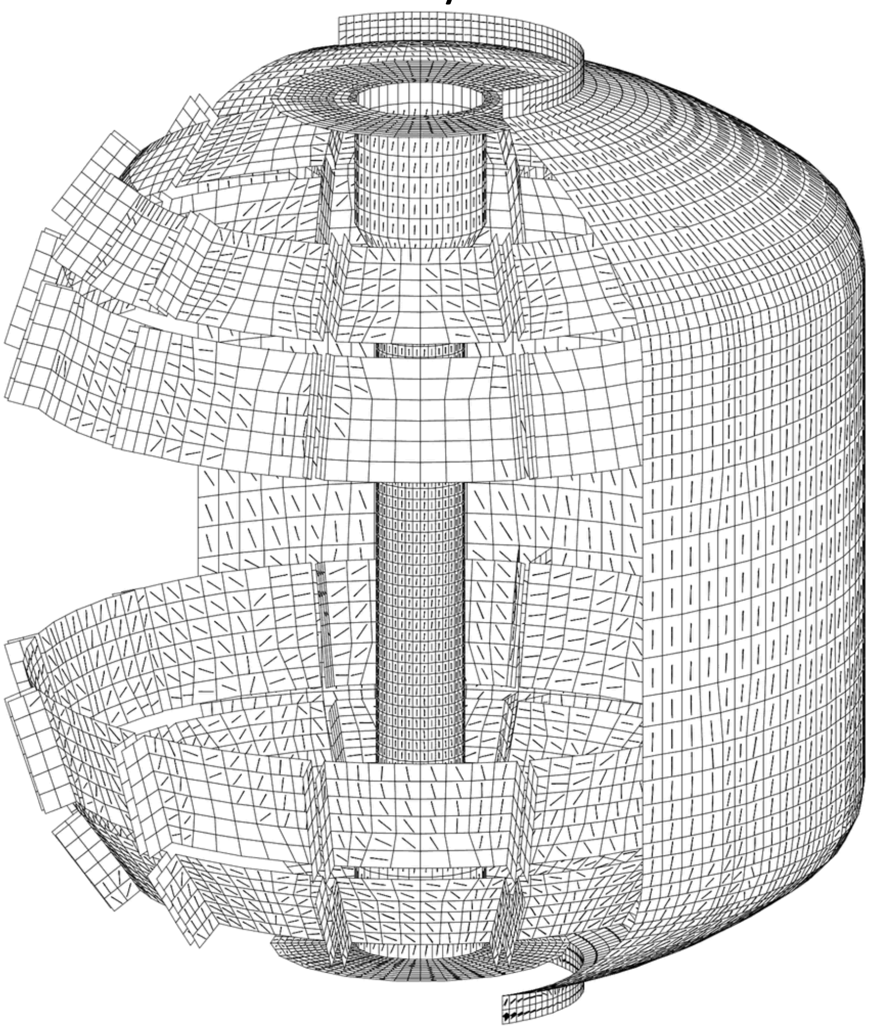

Arrow scale: surface current density up to 492 kA/m

Bottom view

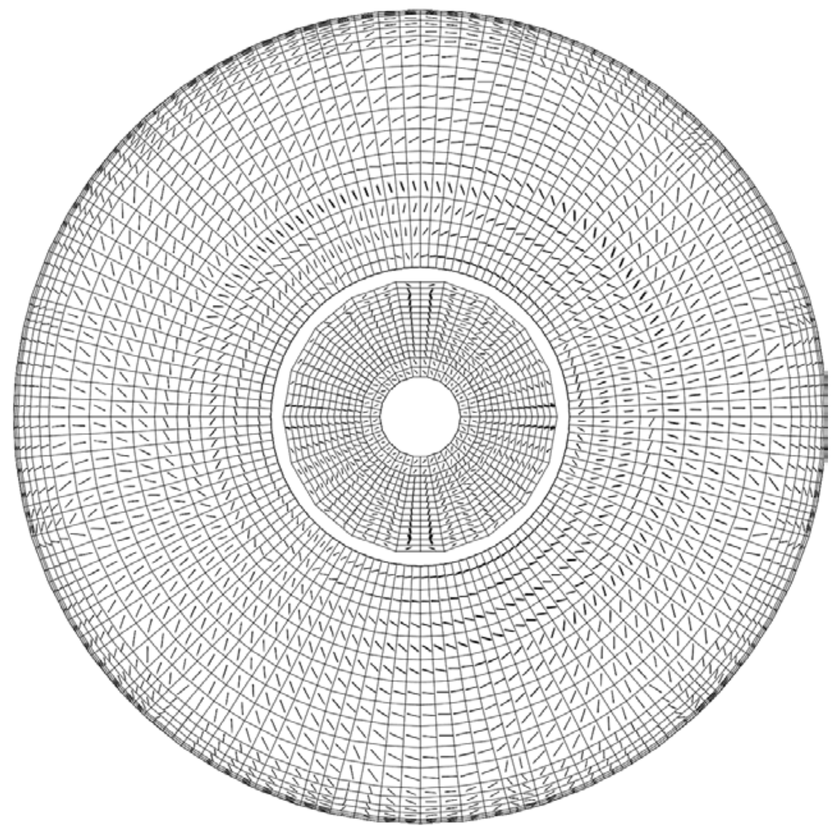

Arrow scale: surface current density up to 517 kA/m

Summary of VDE results

- MHD simulation plausibly accounts for most observed qualitative features of NSTX VDEs, including degree of toroidal peaking.

- Substantial differences exist between 2D and 3D IVB results, suggesting that a more sophisticated 3D model should be used to achieve accuracy in a self-consistent MHD calculation.

Outline

- Verification of M3D with the DSC test problem
  - Equilibrium & stability
  - Nonlinear saturation of free boundary kink
  - Nonlinear saturation of wall-touching kink
- NSTX VDE study
  - Experimental observations
  - M3D results
  - IVB results
- Conclusions

Conclusions

- The validation study provides strong evidence that traditional MHD codes can be useful for disruption halo current calculations.
  - Should be followed up with calculations with the tile wall at the mesh boundary.
  - The 3D DSC code should be able to reproduce the vacuum bubble result.

- The NSTX VDE calculations show good qualitative agreement with experiment, but coupling to IVB demonstrates that quantitative prediction may require a 3D thick wall model.
  - M3D-C1 now implements such a model and should be used for follow-up work.
  - Forthcoming IVB calculations using dI/dt coupling to get eddy currents should provide further insight.

Extra Slides

Current sheet resolution (detail)

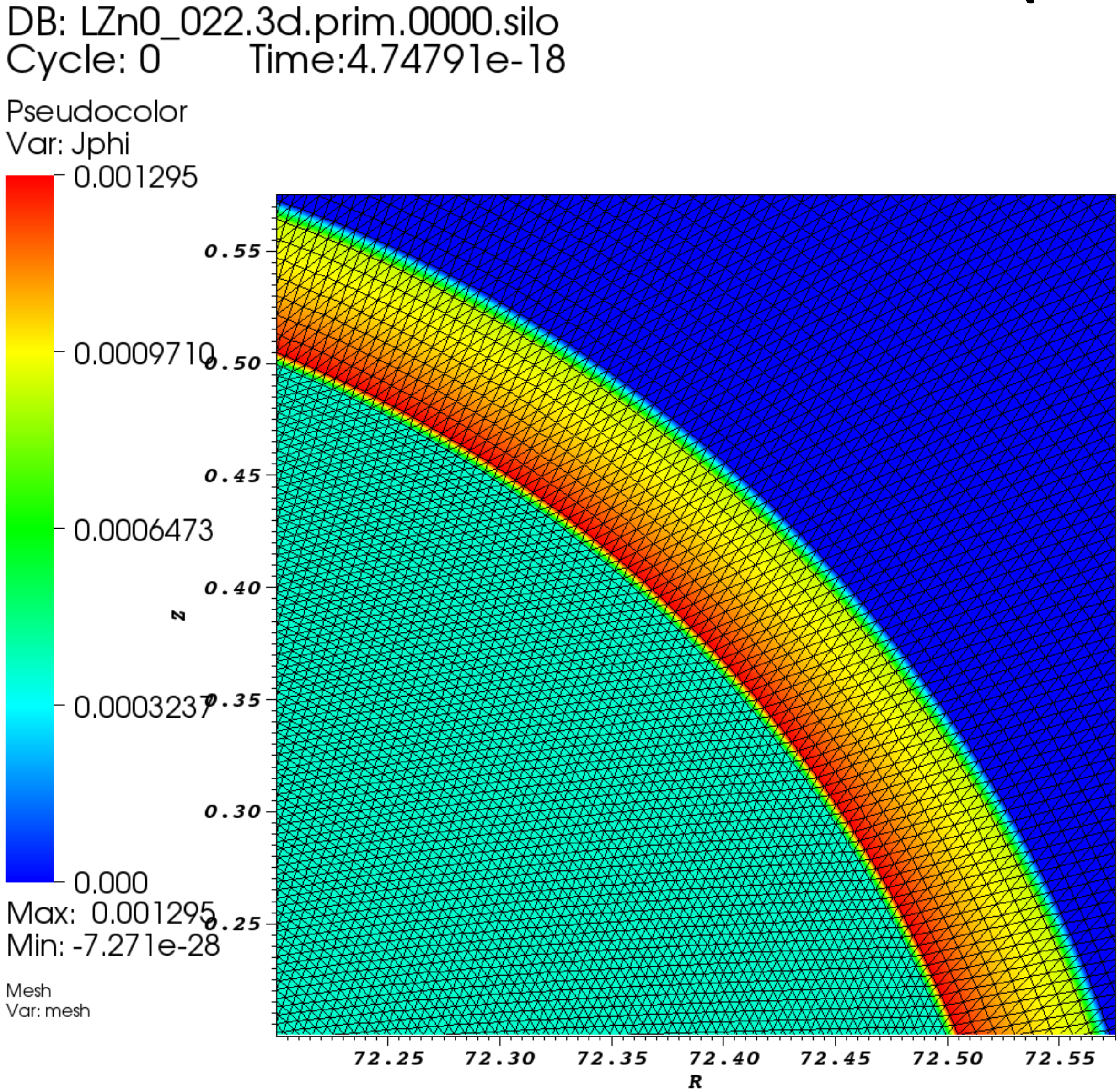

Higher *n* modes

n=2 eigenmode

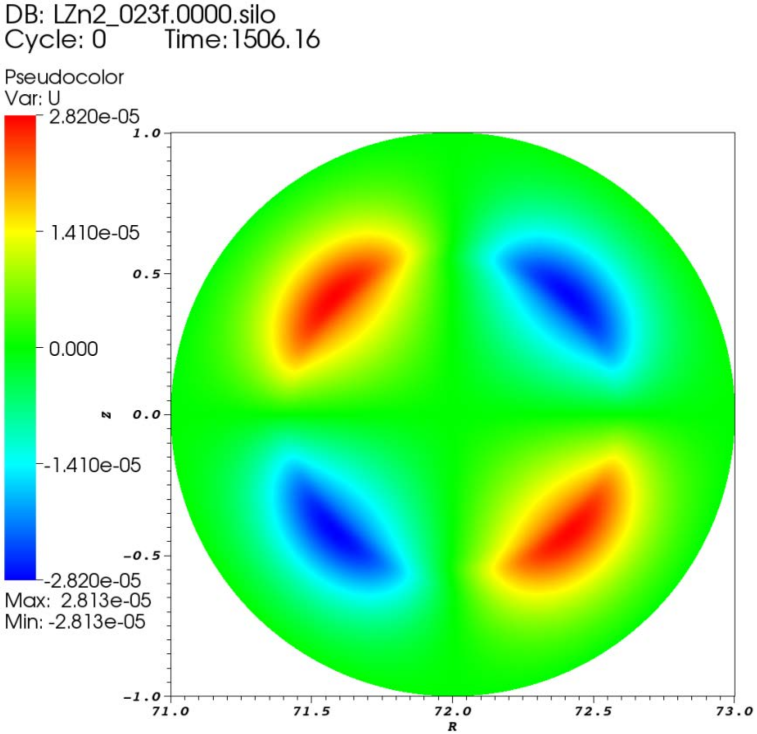

$\gamma\tau_A$ = 0.00368 $\pm$ 0.00043 (htor=0.001);
$\gamma\tau_A$ = 0.00832 $\pm$ 0.00004 (htor=0.0)

n=3 eigenmode

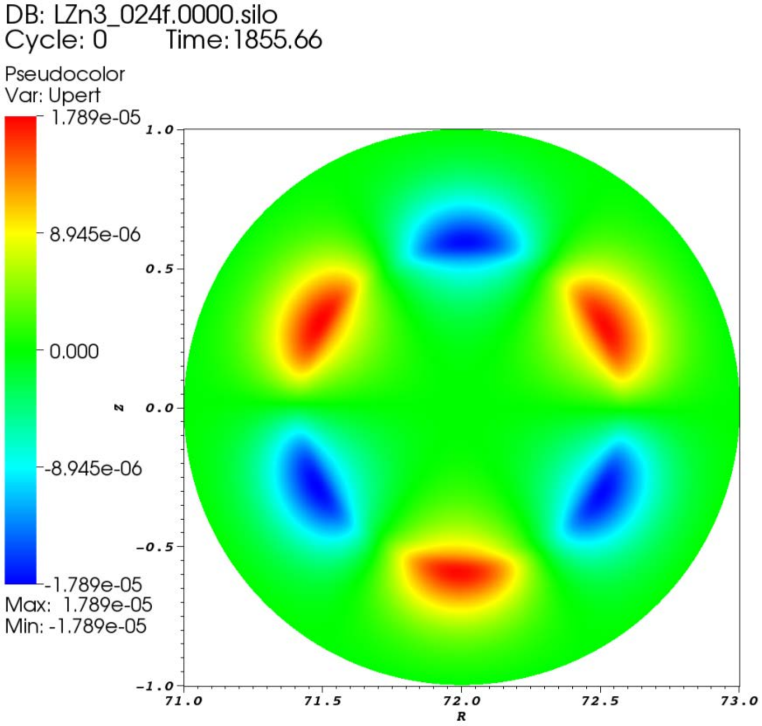

$\gamma\tau_A$ = 0.0007 $\pm$ 0.0001 (htor=0.001);
$\gamma\tau_A$ = 0.00875 $\pm$ 0.0001 (htor=0.0)

Current evolution during WTK

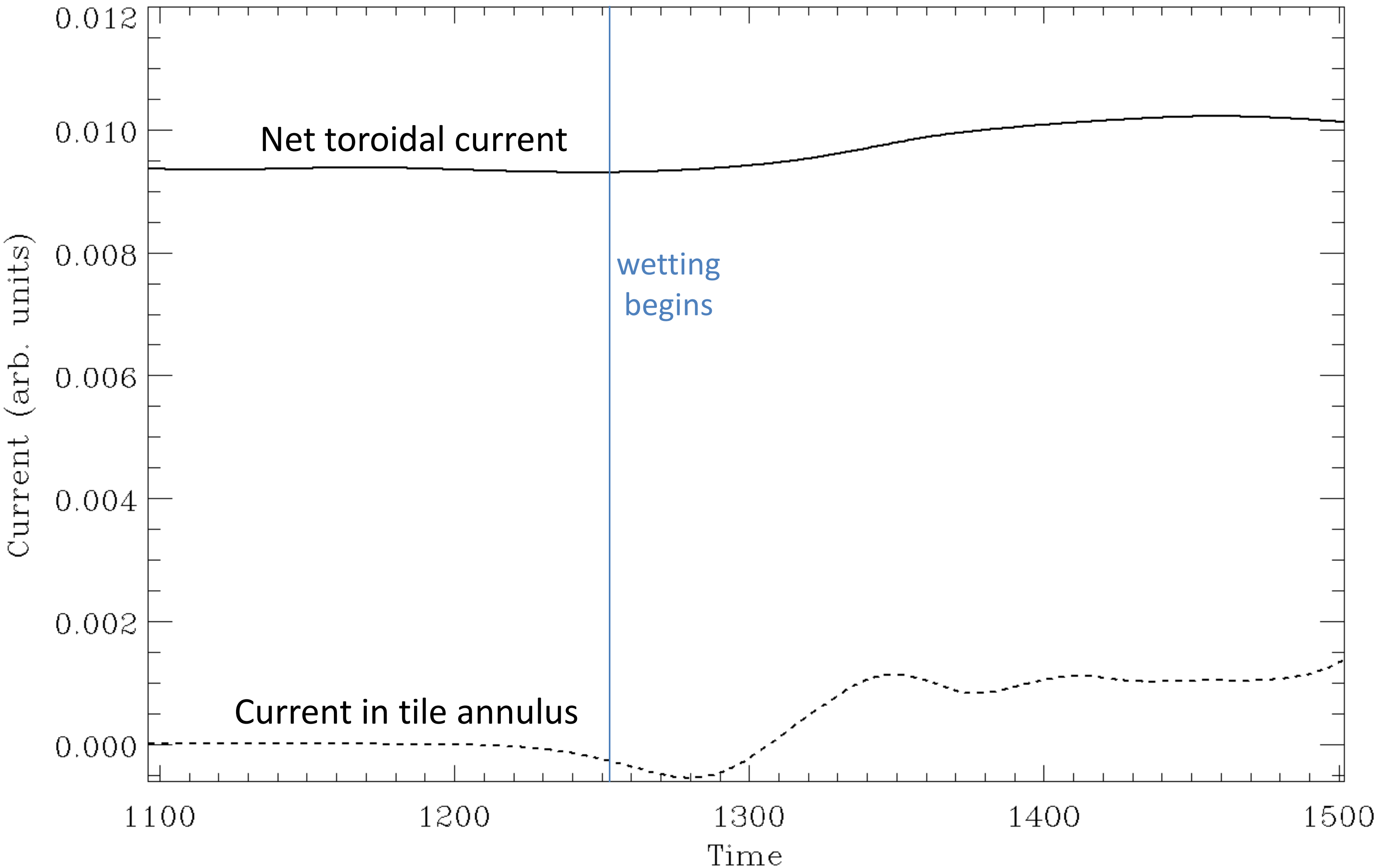

Toroidally Asymmetric Halo Current Figures of Merit

Halo fraction (HF): If there are N poloidal planes, j=1,2,3,…,N, then

$$HF \equiv \frac{\frac{2\pi}{N}\sum_{j=1}^{N}\left\{\oint_{\Gamma_j} R\left|\mathbf{J}\cdot\hat{n}\right|dl\right\}}{I_{p0}},$$

where I_{p0} is the total plasma current in the initial equilibrium.

Toroidal peaking factor (TPF):

$$TPF \equiv \frac{\mathrm{Max}_{j=1}^{N}\left\{\oint_{\Gamma_j} R\left|\mathbf{J}\cdot\hat{n}\right|dl\right\}}{\frac{1}{N}\sum_{j=1}^{N}\left\{\oint_{\Gamma_j} R\left|\mathbf{J}\cdot\hat{n}\right|dl\right\}} = 1 \text{ for axisymmetric halo current}$$

Key Parameters for NSTX VDE calculation

Plasma resistivity on axis* $\eta_0 = S^{-1}$	5×10^{-8}
η_{vacuum} / η_0	3333
η_{wall} / η_0	2000 (τ_w / τ_A=10,000)
Prandtl number μ / η_0	10
Perpendicular heat conduction $\kappa_\perp / \eta_0$	200
Parallel heat conduction $\kappa_{\|\|} / \eta_0$	2,000,000
Density evolution	Off (uniform, constant)
Size of initial n=1 perturbation (post-2D)	10^{-6}
Number of toroidal modes	12

Time History (nonlinear 2D VDE phase)

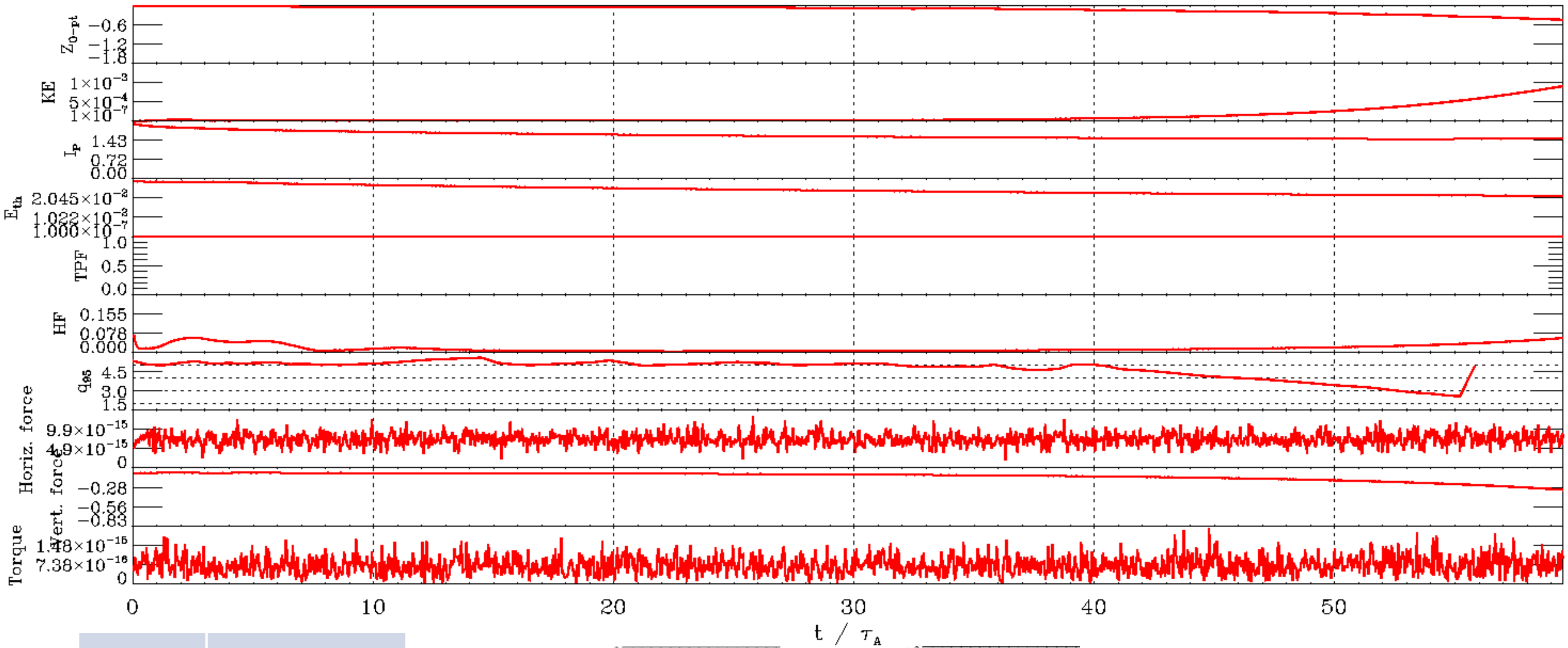

η_0	6×10^{-5}
η_{vac}	2×10^{-1}
η_{wall}	1.2×10^{-1}
μ_0	6×10^{-4}
μ_{edge}	1.2×10^{-1}
$\kappa_\perp$	10^{-5}
$\kappa_{\|\|}$	10^{-1}

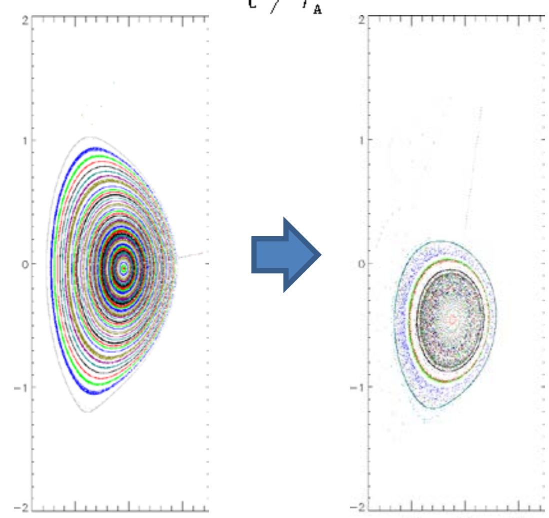

q_{95} is projected to reach 2.0 at t=58.7 (about seven wall times).

IVBRANCH

a code to explore halo current distributions
in arbitrary conducting structures

J. Bialek APAM Columbia University October 25, 2013

$$\begin{bmatrix} [L] & [0] \\ [N]^t & [0] \end{bmatrix} \begin{Bmatrix} \{\dot{I}(t)\} \\ \{\dot{\phi}(t)\} \end{Bmatrix} + \begin{bmatrix} [R] & [N] \\ [0] & [0] \end{bmatrix} \begin{Bmatrix} \{I(t)\} \\ \{\phi(t)\} \end{Bmatrix} = \begin{Bmatrix} \{b(t)\} \\ \{\dot{f}(t)\} \end{Bmatrix}$$

where :

$\{I(t)\}_{Bx1}$ = branch currents (tbd)

$\{\phi(t)\}_{Nx1}$ = node voltages (tbd)

$[L]_{BxB}$ = branch by branch inductance matrix

$[R]_{BxB}$ = branch by branch resistance matrix

$[N]_{BxN}$ = edge node incidence matrix

$\{b(t)\}_{Bx1}$ = branch voltage (exterior sources)

$\{f(t)\}_{Nx1}$ = nodal flows (exterior sources)

model conducting structures with 1-D, 2-D, & 3-D elements, end up with N 'nodes' & B 'branches' in model

user defines:

1) exterior magnetic d(B)/dt
2) surface normal current density
3) reference nodal voltage(s) in model

code solves for:
current and voltage in model